Periodic Oscillations for Non Monotonic Smooth Negative Feedback Circuits

Camille Poignard, Madalena Chaves, Jean-Luc Gouzé

SIAM J. APPLIED DYNAMICAL SYSTEMS
Vol. xx, pp. x

PERIODIC OSCILLATIONS FOR NON MONOTONIC SMOOTH NEGATIVE FEEDBACK CIRCUITS*

Camille Poignard*†, Madalena Chaves*‡, and Jean-Luc Gouzé*§

Abstract. Negative feedback circuits are a recurrent motif in regulatory biological networks, strongly linked to the emergence of oscillatory behavior. The theoretical analysis of the existence of oscillations is a difficult problem and typically involves many constraints on the monotonicity of the activity functions. Here, we study the occurrence of periodic solutions in an n-dimensional class of negative feedback systems defined by smooth vector fields with a window of not necessarily monotonic activity. Our method consists in circumscribing the smooth system by two piecewise linear ones, each admitting a periodic solution. It can then be shown that the smooth negative feedback system also has a periodic orbit, inscribed in the topological solid torus constructed from the two piecewise linear orbits. The interest of our approach lies in: first, adopting a general class of functions, with a non monotonicity window, which permits a better fitting between theoretical models and experimental data, and second, establishing a more accurate location for the periodic solution, which is useful for computational purposes in high dimensions. As an illustration, a model for the "Repressilator" synthetic system is analyzed and compared to real data, and shown to admit a periodic orbit, for a range of activity functions.

Key words. Piecewise linear systems; negative feedback circuits; periodic oscillations; Poincaré maps

AMS subject classifications. 34, 92

1. Introduction.

The investigation of the dynamical features of small regulatory units has been growing in interest for several decades, motivated by the necessity of controlling and predicting the global behaviors of biological organisms (see [39, 41]). Many mathematical tools have been developed for this purpose, leading to several types of modeling frameworks in Systems and Synthetic Biology ([30, 24, 3, 42, 32]). Here we are interested in the link between continuous models (where the variations of concentrations in the molecules are represented by ordinary differential equations) and piecewise linear models as introduced by L. Glass in [14] (see [15, 17, 8]), where the equations combine piecewise constant production terms with linear degradation. The setting of piecewise linear models for biological systems has been widely studied during the last decades, as it provides useful analytical tools and explicit formulae of the solutions: for instance we refer the reader to [17, 26, 6, 1, 4, 29, 43] for an idea of the advances made since the work initiated by L. Glass, and to [10, 5] for experimental validations of some of the results found theoretically. A useful direction in this field is to construct an approximation of a given system of ordinary differential equations by a piecewise linear system (in an appropriate state space grid) thus obtaining a simplified model for further theoretical

*This work was supported in part by the projects GeMCo (ANR 2010 BLANC020101), RESET (Investissements d'Avenir, Bioinformatique, ANR-11-BINF-0005), and by the LABEX SIGNALIFE (ANR-11-LABX-0028-01).This is an author version.

*Inria, Biocore, Sophia Antipolis-Méditerranée, BP 93, 06 902 Sophia Antipolis, France
†camille.poignard@inria.fr
‡madalena.chaves@inria.fr
§jean-luc.gouze@inria.fr

analysis and simulations [3, 43, 32]. Our purpose here is not to develop new tools for piecewise linear models but to use them so as to deduce novel results concerning continuous ones.

Periodic oscillations are ubiquitous in biological organisms, both in natural cellular signalling pathways ([33, 35, 22]) and in synthetically designed networks ([5, 9, 38]). Thanks to the tools of dynamical systems theory, the mechanisms leading to periodic oscillations or mixed mode oscillations have been unveiled quite successfully (as can be seen by circadian rhythms [2, 25], or mammalian cell cycle). In the continuous setting, among the vast literature concerning negative feedback circuits, let us mention the early model of Goodwin [18] in the context of enzyme kinetics, the work of J. J. Tyson [40] who proved the existence of large amplitude oscillations for the cyclic negative feedback system of J. S. Griffith [19] in three dimensions, and also S. P. Hastings [20] who improved this result for a modified version of this model with a step function, by giving uniqueness and stability of the limit cycle. Their results were generalized by H. L. Smith [37] for competitive or cooperative systems.

However, in the case of networks with a high number of components, the existence of periodic oscillations in continuous models is in general difficult to establish rigorously. Most of the known results are heavily based on monotonicity of the system (as in [21] where other stability properties are assumed). J. Mallet-Paret and H. L. Smith obtained a strong result on monotone cyclic feedback systems ([27, 28]), showing their dynamics can be reduced to $\mathbb{R}^2$ and are thus described by the Poincaré-Bendixson Theorem, excluding by the way chaotic behaviors for such models (contrary to other genetic regulatory models like in [31]). Another class of general, smooth, cyclic feedback systems is also studied by T. Gedeon and K. Mischaikow [11, 13], where techniques from Conley Theory and Morse sets are used to establish several dynamical properties. In particular, [11] constructs a system (essentially a linear cycle with a single nonlinear term) that may exhibit chaotic dynamics. In other works the use of slow-fast dynamics hypotheses is required (such as in [12]). Lastly, the location of these oscillations are often difficult to identify.

The present work goes in this direction: our goal is to establish the existence of periodic oscillations in (non monotonic) smooth systems using piecewise linear approximations, that will in turn provide an approximation of the periodic orbit of the original smooth system.

A similar idea was formulated by L. Glass and J. S. Pasternack in the 70's. In Conjecture 3 of [16], they claimed the following:
If there is a limit cycle attractor for a PL (piecewise linear) *system then there will be a limit cycle attractor for a continuous homologue, [...]. The cycle in the continuous system will approximate the cycle in the PL system.*

We aim at proving a related result for a class of (smooth) negative feedback circuits, where our contribution consists in admitting a class of non-monotonic functions and establishing a well defined locus for the periodic solutions. Considering a simple negative feedback loop with n variables, we will show the existence of a Poincaré section for the (smooth) differential system associated with this model Σ^μ, by studying the periodic orbits of two piecewise linear systems which circumscribe Σ^μ (one "interior" system and one "exterior"). Namely, the nonlinear functions defining the equations of Σ^μ are bounded below and above by two step functions and by a suitable combination of these bounds for each variable, "interior" and "exterior"

piecewise linear systems can be generated. The nonlinear functions defining our model are required to be continuous (or smooth) and equal to the step functions except in a narrow interval $[\theta - \delta, \theta + \delta]$ around the threshold θ where the step function jumps from 0 to 1. In this interval, the nonlinear functions are unknown and can be monotonic or not.

A similar approach was also investigated in a different way in [36], but the models considered are two-dimensional and concern a hybrid systems setting where the continuous system is completely known: here we don't require explicit knowledge of the full system.

The fact monotonicity is not required on the nonlinear functions defining the model is one of the advantages of our approach, compared to the other works mentioned above: however, one will notice the non monotone part of the functions is restricted to a small window of size 2δ. In addition, the value δ should remain small enough to avoid breaking the negative loop structure.

The other main interest of our method lies in the fact it permits to control the size of the invariant toroïdal neighborhood containing (at least one) periodic orbit, which corresponds to the size δ of the window in which the equations of our model are unknown. Moreover, this invariant topological solid torus is itself constructed from the periodic orbits of the interior and the exterior piecewise linear models. As a consequence, these two orbits give a good approximation of the periodic oscillations of the continuous model, which is numerically of interest as they are easier to compute.

The rest of the paper is organized as follows. The first five parts are dedicated to the proof of our result in dimension $n = 3$: indeed, the exactly same reasoning applies to the case $n \geq 3$, which is explained in Section 6 at the end of the paper. In section 2 we first recall the basics of the piecewise linear setting. Then we define the different three-dimensional models (differential, piecewise linear) that will be dealt with in the paper. In section 3 we present the exterior and the interior piecewise linear systems defined in order to bound our continuous model, and prove the existence of a Poincaré invariant section for the interior system, that therefore admits a periodic orbit γ^- (see Lemma 3.5). By the same reasoning we show that the exterior piecewise linear system has a periodic trajectory γ^+ (Lemma 3.9). It becomes clear from the proofs that γ^- is indeed interior to γ^+. From this we prove in Section 4 the existence of a Poincaré section for the three-dimensional differential model (Theorem 4.1), delimited by the impact points of γ^- and γ^+ inside the plane containing this section. To illustrate our modeling framework, in Section 5, the method is applied to the "Repressilator" systems ([5]), a biological example of a negative feedback circuit which exhibits oscillations. Based on experimental data from [5], we obtain physiological parameters that satisfy our conditions. Numerical simulations show the periodic orbit γ^μ of the model defined by these parameters, and the torus bounded by the two orbits γ^- and γ^+ in which is inscribed γ^μ. Lastly, as mentioned previously the last part (Section 6) contains the extension of our result to dimension $n \geq 3$.

2. Basic notations and definitions.

2.1. The differential system $\Sigma^\mu_{\theta,k,\gamma,\delta}$. Throughout the paper $\mathbb{R}_+ = [0, +\infty[$ denotes the set of positive real numbers including zero. Our study focuses on negative feedback networks of the form (-,+,+) (or of the form (-,+,...,+) for the n-dimensional case, see Section 6), that is to say on networks with three genes A_1, A_2, A_3 (of which concentrations will be denoted

x_1, x_2, x_3 below) forming a loop with two negative feedbacks and a positive one, which is represented by the interaction graph of Figure 1.

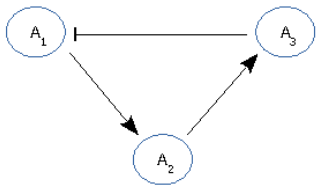

Figure 1. *The negative feedback loop (-,+,+). In this picture, an edge terminating with a blunt segment (respectively an arrow) represents an inhibition (respectively an activation) of transcription.*

Negative feedback loops appear frequently in gene regulatory networks ([5, 6, 14, 21, 40]). Based on gene expression data, commonly used inhibition or activation functions include monotone Hill type functions [5] or step functions [14]. Here we propose a new class of functions, denoted μ, which admit an interval where the dynamics is unknown, to better account for uncertainty or variability in data parameters. We next give mathematical definitions of our systems.

Notation 2.1. *Given a strictly positive number θ, let $s^+(\cdot,\theta) : \mathbb{R}_+ \to \{0,1\}$ denote the increasing step function defined by the threshold θ, i.e:*

$$\begin{cases} s^+(z,\theta) &= 0 \text{ if } z < \theta \\ s^+(z,\theta) &= 1 \text{ if } z > \theta \end{cases},$$

and by $s^-(\cdot,\theta)$ the decreasing one, defined by the relation $s^-(\cdot,\theta) = 1 - s^+(\cdot,\theta)$.

Our study will focus on the following class of three-dimensional continuous models (see Section 6 for the generalization to higher dimension):

Notation 2.2. *Given a real number $\delta > 0$, let $\Sigma^{\mu}_{\theta,k,\gamma,\delta}$ denote the following ordinary differential system in $\mathbb{R}^3$:*

$$\Sigma^{\mu}_{\theta,k,\gamma,\delta} : \begin{cases} \dot{x_1} &= k_1\mu^-(x_3,\theta_3,\delta) - \gamma_1 x_1 \\ \dot{x_2} &= k_2\mu^+(x_1,\theta_1,\delta) - \gamma_2 x_2 \\ \dot{x_3} &= k_3\mu^+(x_2,\theta_2,\delta) - \gamma_3 x_3 \end{cases},$$

where the functions $\mu^-(\cdot,\theta,\delta) : \mathbb{R}_+ \to [0,1]$ and $\mu^+(\cdot,\theta,\delta) : \mathbb{R}_+ \to [0,1]$ are continuous or smooth functions coinciding with $s^-(\cdot,\theta)$ and $s^+(\cdot,\theta)$, except in a narrow window of size 2δ around the threshold θ where they can be monotonic or not, i.e:

$$\mu^+(x) : \begin{cases} 0, \text{ if } x \leq \theta - \delta \\ \overline{\mu^+}(x), \text{ if } \theta - \delta \leq x \leq \theta + \delta \\ 1, \text{ if } \theta + \delta \leq x \end{cases},$$

where $\overline{\mu^+}$ is at least $\mathcal{C}^1$ and satisfies $\overline{\mu}(\theta - \delta) = 0$ and $\overline{\mu}(\theta + \delta) = 1$ (see Figure 2). Similarly for μ^-.

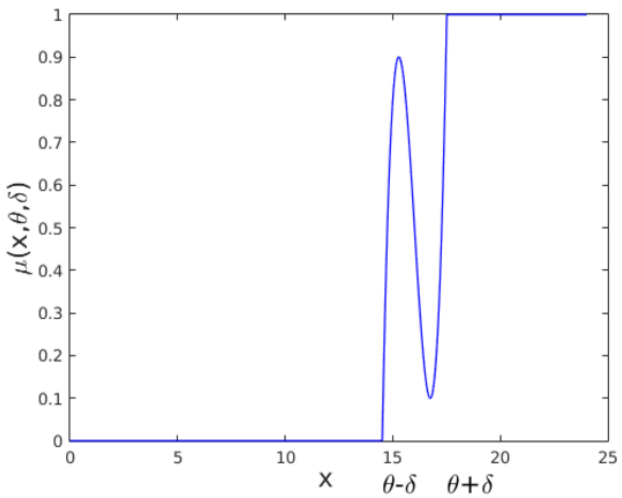

Figure 2. *An example of the function $\mu(\cdot, \theta, \delta)$. The non monotonic part of $\mu(\cdot, \theta, \delta)$ stands in the interval $[\theta - \delta, \theta + \delta]$ (this function will be used later, see Section 5).*

We can say the continuous systems $\Sigma^{\mu}_{\theta,k,\gamma,\delta}$ are *negative* feedback loop models: indeed when x_3 is varying from a value smaller than $\theta_3 - \delta$ to a value greater than $\theta_3 + \delta$, we pass from a full rate production of x_1 to a null one. It is then said that x_3 *inhibits* x_1 (similarly x_1 activates x_2 and x_2 activates x_3), and our continuous model effectively corresponds to the graph shown in Figure 1. This justifies the use of the adjective *negative* to characterize our model (as it is very often done in the literature, see for instance [19, 21, 39]).
Notice that for initial conditions taken in ${\mathbb{R}_+}^3$, the trajectories of this system stay in ${\mathbb{R}_+}^3$, which is consistent with the fact our model represent the evolutions of concentrations in molecules. Besides, all the trajectories are bounded and inscribed in the cube $[0, \frac{k_1}{\gamma_1}] \times [0, \frac{k_2}{\gamma_2}] \times [0, \frac{k_3}{\gamma_3}]$. The proof of these two points (which also stand for the piecewise linear systems we are going to define in Section 3 below) is left to the reader.

To prove the existence of periodic oscillations in this model, our strategy is to compare its dynamics with approximated piecewise linear versions.

2.2. The piecewise linear setting. Let's recall some basic facts about piecewise linear systems (see [6], [14]), for a complete introduction to this subject). The ones we consider have the following form:

$$(\mathcal{S}) \begin{cases} \dot{x_1} & = \kappa_1(x) - \gamma_1 x_1 \\ & \vdots \\ \dot{x_n} & = \kappa_n(x) - \gamma_n x_n \end{cases},$$

where each variable x_i is in $\mathbb{R}^n_+$ and each function $\kappa_i : \mathbb{R}^n_+ \to \mathbb{R}_+$ is an element of the algebra of step functions. More precisely, our functions κ_i will be sums of products of functions of

the form $s^+(\cdot,\theta)$, and $s^-(\cdot,\theta)$. As a consequence, each function κ_i is piecewise constant over $\mathbb{R}^n_+$ and associated with a set of thresholds $\Theta_i = \{\theta_i^1, \cdots, \theta_i^{q_i-1}\}$. As trajectories of $(\mathcal{S})$ are confined in a region of $\mathbb{R}^n_+$, we assume without loss of generality the following family of inequalities:

$$\theta_i^0 = 0 < \theta_i^1 < \cdots < \theta_i^{q_i-1} < \theta_i^{q_i},$$

where $\theta_i^{q_i}$ is a positive bound for the variable x_i. This family partitions the region of $\mathbb{R}^n_+$ (in which the flow evolves) in rectangular domains; the interiors of each of them are boxes called *regular domains* and have the following form:

$$\{x \in \mathbb{R}^n_+ : \forall i \in \{1, \cdots, n\},\ \exists j \in \{0, \cdots, q_i - 1\},\ \theta_i^j < x_i < \theta_i^{j+1}\}.$$

Then, in a given regular domain B, the flow admits a unique equilibrium point usually called *focal point* in the literature(see [1]), namely the point $(k_1(B)/\gamma_1, \cdots, k_n(B)/\gamma_n)$, where $k_i(B)$ stands for the constant value of κ_i in the box B. We will only consider the case where each focal point of a regular domain B is outside B (see the assumptions of Lemma 3.5), in order to prevent from having a trivial asymptotic stationary dynamics in a box, which is not our objective.

Now, as the reader may have noticed it, although the vector field $(\mathcal{S})$ is defined everywhere in $\mathbb{R}^n_+$, its associated flow is not always uniquely defined: indeed on *walls* between the boxes, and more generally on sets of the form $\{x \in \mathbb{R}^n_+ :\ \exists i \in \{1, \cdots, n\},\ x_i \in \Theta_i\}$ usually called *switching domains* in the literature, we generally loose unicity of trajectories. This is the case when the directions of the vector fields in two consecutive boxes are opposite. A setting for rigorously defining "solutions" in such a case has been proposed by A. F. Filippov (see [8]), leading to the notion of set-valued solutions.
Nonetheless, when the vector fields in all regular domains are well directed (notably when the ones of two consecutive boxes are never facing each other), the trajectories in the switching domains between two consecutive regular domains can be extended continuously. In this case, the switching domains are called "transparent walls" (see [6]) in the literature.
In this paper, we will assume that all switching domains are transparent (see the next section).

3. The Exterior System and the Interior System. It is useful to introduce the piecewise linear version of our model $\Sigma^{\mu}_{\theta,k,\gamma,\delta}$, that is the following system $\Sigma_{\theta,k,\gamma}$:

Definition 3.1. *We call piecewise linear three-dimensional negative feedback loop model, the following piecewise linear system in* $\mathbb{R}^3$*:*

$$\Sigma_{\theta,k,\gamma} : \begin{cases} \dot{x_1} &= k_1 s^-(x_3, \theta_3) - \gamma_1 x_1 \\ \dot{x_2} &= k_2 s^+(x_1, \theta_1) - \gamma_2 x_2 \\ \dot{x_3} &= k_3 s^+(x_2, \theta_2) - \gamma_3 x_3 \end{cases}.$$

As said in the introduction, our idea is to circumscribe in some sense the continuous model $\Sigma^{\mu}_{\theta,k,\gamma,\delta}$ by two piecewise linear systems (both from the inside and from the outside), each of these admitting a periodic piecewise linear orbit.

Let's explain heuristically how these two models are constructed. As the function $\mu^+(\cdot, \theta_i, \delta)$ is bounded from below by $s^+(\cdot, \theta_i + \delta)$ and bounded from above by $s^+(\cdot, \theta_i - \delta)$ (and similarly for $\mu^-(\cdot, \theta_i, \delta)$), our idea is to consider extended versions of $\Sigma_{\theta,k,\gamma}$ when the threshold θ_i is replaced by the two thresholds $\theta_i - \delta$ and $\theta_i + \delta$ (which leads to a separation of the state space in 3^3 regular domains instead of 2^3). To construct these extended systems we proceed in the following way: consider a switching domain for $\Sigma_{\theta,k,\gamma}$, of the form $x_i = \theta_i$, separated by two regular domains, say B^- (defined by a vector field f^-) on the left of this wall, and B^+ (defined by f^+) on the right. Let us look at the orbits passing from B^+ to B^- (for the ones passing from B^- to B^+ we proceed similarly): they are first defined by f^+ and then by f^-. Now that we have another box (defined by the relation $\theta_i - \delta < x_i < \theta_i + \delta$) inserted between B^+ and B^-, we have naturally two possibilities for a trajectory reaching the wall $x_i = \theta_i + \delta$: we can either consider the continuation of this trajectory according to f^+, or change immediately and start following f^-. Intuitively, in every box, the trajectories of the differential system Σ^μ are inscribed in the region defined by these two possibilities. The definition of the exterior (respectively interior) system is based on the choice of the first (respectively second) possible extension in each box. This idea is illustrated in Figure 3, which shows the projection on the plane x_1, x_2 of the three-dimensional exterior, interior, and continuous systems (denoted by Σ^+, Σ^-, and Σ^μ in this figure). All trajectories start from the same point and follow the same vector fields *outside* the regions $\theta_i - \delta < x_i < \theta_i + \delta$. On reaching a wall $x_i = \theta_i \pm \delta$, trajectories of Σ^+ continue following the same vector field (red curves), trajectories of Σ^- change immediately (blue curves) and Σ^μ follows its own field μ.

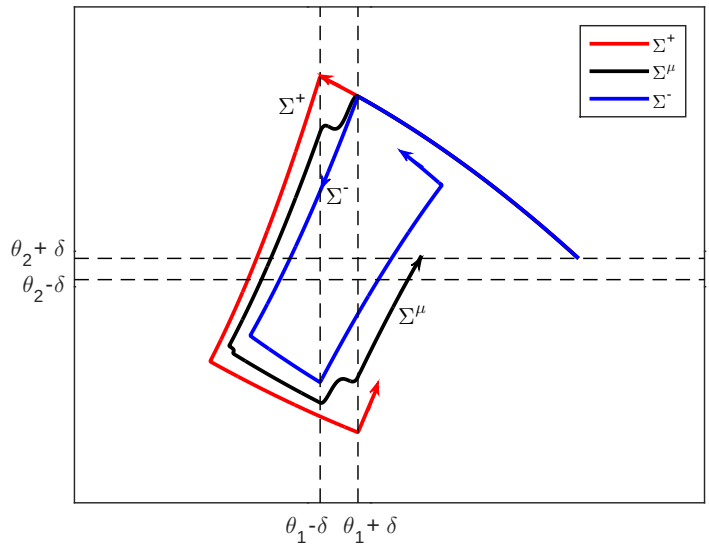

Figure 3. *Representation of the construction of the exterior and interior piecewise linear systems. Projection on the plane x_1, x_2 of the trajectories of Σ^+, Σ^-, and Σ^μ. For an example of limit cycle of Σ^μ bounded by limit cycles of Σ^- and Σ^+ see Figure 8 and Figure 7.*

Here is the precise definition of the exterior and the interior systems, respectively denoted

by $\Sigma^{+}_{\theta,k,\gamma,\delta}$ and $\Sigma^{-}_{\theta,k,\gamma,\delta}$:

Notation 3.2. *We call "exterior system" the following piecewise-linear system, denoted by* $\Sigma^{+}_{\theta,k,\gamma,\delta}$*:*

$$\Sigma^{+}_{\theta,k,\gamma,\delta}: \begin{cases} \dot{x_1}(t) = k_1\left(s^-(x_3,\theta_3+\delta)\,s^+(x_1,\theta_1+\delta)+s^-(x_3,\theta_3-\delta)\,s^-(x_1,\theta_1+\delta)\right)-\gamma_1 x_1 \\ \dot{x_2}(t) = k_2\left(s^+(x_1,\theta_1+\delta)\,s^-(x_2,\theta_2+\delta)+s^+(x_1,\theta_1-\delta)\,s^+(x_2,\theta_2+\delta)\right)-\gamma_2 x_2 \\ \dot{x_3}(t) = k_3\left(s^+(x_2,\theta_2+\delta)\,s^-(x_3,\theta_3+\delta)+s^+(x_2,\theta_2-\delta)\,s^+(x_3,\theta_3+\delta)\right)-\gamma_3 x_3 \end{cases},$$

and "interior system" the following one, denoted by $\Sigma^{-}_{\theta,k,\gamma,\delta}$*:*

$$\Sigma^{-}_{\theta,k,\gamma,\delta}: \begin{cases} \dot{x_1}(t) = k_1\left(s^-(x_3,\theta_3-\delta)\,s^+(x_1,\theta_1+\delta)+s^-(x_3,\theta_3+\delta)\,s^-(x_1,\theta_1+\delta)\right)-\gamma_1 x_1 \\ \dot{x_2}(t) = k_2\left(s^+(x_1,\theta_1-\delta)\,s^-(x_2,\theta_2+\delta)+s^+(x_1,\theta_1+\delta)\,s^+(x_2,\theta_2+\delta)\right)-\gamma_2 x_2 \\ \dot{x_3}(t) = k_3\left(s^+(x_2,\theta_2-\delta)\,s^-(x_3,\theta_3+\delta)+s^+(x_2,\theta_2+\delta)\,s^+(x_3,\theta_3+\delta)\right)-\gamma_3 x_3 \end{cases}.$$

Both of these two systems $\Sigma^{-}_{\theta,k,\gamma,\delta}$, $\Sigma^{+}_{\theta,k,\gamma,\delta}$ reduce to $\Sigma_{\theta,k,\gamma}$ for $\delta=0$.

Notation 3.3. *Let* $B_{a_1a_2a_3}$ *denote each of the* 27 *regular domains associated with the systems* $\Sigma^{+}_{\theta,k,\gamma,\delta}$ *and* $\Sigma^{-}_{\theta,k,\gamma,\delta}$*, where the tuples* (a_1,a_2,a_3) *belong to* $\{0,1,2\}^3$*, and are defined by:*

$$\forall\ 1\le i\le 3,\ a_i=\begin{cases} 0 \text{ if } & 0<x_i<\theta_i-\delta \\ 1 \text{ if } & \theta_i-\delta<x_i<\theta_i+\delta \\ 2 \text{ if } & \theta_i+\delta<x_i \end{cases}.$$

In each of these boxes, the trajectories of the two piecewise linear systems $\Sigma^{-}_{\theta,k,\gamma,\delta}$ and $\Sigma^{+}_{\theta,k,\gamma,\delta}$ can be easily computed. Namely, in each regular domain $B_{a_1a_2a_3}$ and for every integer $1\le i\le 3$, the ith component of $\Sigma^{-}_{\theta,k,\gamma,\delta}$ has either the expression:

$$\dot{x_i}=-\gamma_i x_i \text{ (which yields } x_i(t)=e^{-\gamma_i t}x_i(0))$$

or

$$\dot{x_i}=k_i-\gamma_i x_i \text{ (which yields } x_i(t)=\frac{k_i}{\gamma_i}+e^{-\gamma_i t}\left(x_i(0)-\frac{k_i}{\gamma_i}\right)).$$

In the first case the component $x_i(t)$ decreases in time, while in the second case it is increasing. The same holds for the exterior system $\Sigma^{+}_{\theta,k,\gamma,\delta}$.

3.1. Existence of a periodic orbit for the Interior System. We first establish the existence of a periodic orbit for the interior system $\Sigma^{-}_{\theta,k,\gamma,\delta}$: to do this we prove it admits a Poincaré section under some conditions on its parameters (Lemma 3.5 below). As there are several definitions possible for a Poincaré section, let us precise what we mean by this term:

Definition 3.4. *Given a dynamical system* $\dot{x}=\mathrm{g}(x)$ *(where* g *is regular or piecewise linear as in our setting), let* (Σ) *be a hypersurface of its phase space. Then, we say that* (Σ) *is a*

Poincaré section of the flow φ of this system if for every x in (Σ), there exists a time $\tau(x) > 0$ such that the trajectory $(\varphi_t(x))_{t\geq 0}$ crosses transversally the section (Σ) at $\tau(x)$. In this case the map P defined by $\mathrm{P}(x) := \varphi_{\tau(x)}(x) \in (\Sigma)$ is called the "Return map" associated with the Poincaré section (Σ).

Throughout the paper, we will focus more particularly on the case where the section (Σ) is a convex compact set. Indeed, as the map P is continuous (by continuity of the flow) the Brouwer fixed point theorem ([23]) ensures in this case the existence of a fixed point for P in (Σ), that is to say of a periodic orbit for the system considered. This periodic orbit is inscribed in the invariant solid torus generated by the images of the invariant section Σ under the flow φ.

Lemma 3.5. *Let $\eta > 0$ a real number, and let us assume the parameters k_i, γ_i, θ_i satisfy the following condition:*
For every $1 \leq i \leq 3$, $\theta_i > 0$ and $\dfrac{k_2}{\gamma_2} > \theta_2 + \eta$, $\dfrac{k_3}{\gamma_3} > \theta_3 + \eta$.
Then, there exists a real number $\Lambda_0 > \eta$ and a number $\delta_0 > 0$ satisfying the inequality $\delta_0 < \min_{1\leq i\leq 3}(\theta_i, \dfrac{k_i}{\gamma_i} - \theta_i, 1)$ such that, for every $\dfrac{k_1}{\gamma_1} > \Lambda_0 + \theta_1$ and every $0 < \delta \leq \delta_0$, the associated interior system $\Sigma^-_{\theta,k,\gamma,\delta}$ admits the following closed set

$$(\mathcal{P}) : \begin{cases} \dfrac{k_1}{\gamma_1} & \geq x_1 \geq \theta_1 + \eta \\ \dfrac{k_2}{\gamma_2} & \geq x_2 \geq \theta_2 + \delta \\ x_3 & = \theta_3 - \delta \end{cases}$$

as a Poincaré section. The trajectories starting in $(\mathcal{P})$ follow the cycle $\mathcal{C}$ defined by:

$$\mathcal{C} : \begin{array}{ccccccccccc} B_{222} & \to & B_{122} & \to & B_{022} & \to & B_{012} & \to & B_{002} & \to & B_{001} \\ \uparrow & & & & & & & & & & \downarrow \\ B_{221} & \leftarrow & B_{220} & \leftarrow & B_{210} & \leftarrow & B_{200} & \leftarrow & B_{100} & \leftarrow & B_{000} \end{array},$$

while staying outside from the cube $\mathcal{C}_\delta = [\theta_1 - \delta, \theta_1 + \delta] \times [\theta_2 - \delta, \theta_2 + \delta] \times [\theta_3 - \delta, \theta_3 + \delta]$ around the point $(\theta_1, \theta_2, \theta_3)$.

Remark 3.6.

1. *If the assumptions are not satisfied, there exists some sets of parameters for which numerical simulations show the system $\Sigma^-_{\theta,k,\gamma,\delta}$ admits a global equilibrium point, and thus does not have any periodic orbit.*
2. *Moreover, even under the conditions required in Lemma 3.5, it can happen there exists a fixed point inside the cube $\mathcal{C}_\delta$ around $(\theta_1, \theta_2, \theta_3)$. For this reason we look for a Poincaré section far from $\mathcal{C}_\delta$. This is done thanks to the introduction of the new parameter η.*
3. *As could have been expected, the Lemma requires that δ must be small enough compared to the parameters θ_i, in order to remain close to the classical situation with $\delta = 0$ (for*

which we know the existence of a limit cycle, see [6]). Moreover, only the ratio for one variable (namely $\frac{k_1}{\gamma_1}$*) is required to be large enough: by symmetry of the equations, we could have required another ratio to be large.*

Proof. We refer the reader to the Appendix for the proof of this lemma. ■

Now, since this Poincaré section $(\mathcal{P})$ is a rectangular closed set, and its return function continuous, we have by the Brouwer fixed point theorem:

Corollary 3.7. *Under the assumptions of Lemma 3.5 on the parameters* k_i, γ_i, θ_i *and* δ*, there exists a periodic orbit* γ^- *for the interior system* $\Sigma^-_{\theta,k,\gamma,\delta}$*. Moreover, this orbit follows the path given by the cycle* $\mathcal{C}$ *and never crosses the cube* $\mathcal{C}_\delta$*.*

3.2. Existence of a Poincaré section for the exterior system. The next step in the analysis of the system $\Sigma^\mu_{\theta,k,\gamma,\delta}$ is to establish the existence of a periodic orbit for the exterior system $\Sigma^+_{\theta,k,\gamma,\delta}$. To do this we notice the boxes of the cycle $\mathcal{C}$ can be classified in two groups:

Lemma 3.8. *Let* $B_{a_1a_2a_3}$ *a regular domain of the cycle* $\mathcal{C}$*.*
(i) If all the a_i *are distinct from* 1*, then the flows* ϕ^+_t *and* ϕ^-_t *of* $\Sigma^+_{\theta,k,\gamma,\delta}$ *and* $\Sigma^-_{\theta,k,\gamma,\delta}$ *coincide in* $B_{a_1a_2a_3}$*.*
(ii) If there exists an integer $1 \leq i \leq 3$ *such that* $a_i = 1$*, then* ϕ^+_t *and* ϕ^-_t *are different in* $B_{a_1a_2a_3}$*. In this case for both of these flows the trajectories starting from the switching domain* $x_i = \theta_i + \delta$ *reach* $x_i = \theta_i - \delta$ *(respectively the ones starting from* $x_i = \theta_i - \delta$ *reach* $x_i = \theta_i + \delta$*) at a same hitting time* s^d_i *(respectively* s^c_i*):*

$$s^d_i = \frac{-1}{\gamma_i} \ln\left(\frac{\theta_i - \delta}{\theta_i + \delta}\right) \text{ and } s^c_i = \frac{-1}{\gamma_i} \ln\left(\frac{\frac{k_i}{\gamma_i} - \theta_i - \delta}{\frac{k_i}{\gamma_i} - \theta_i + \delta}\right).$$

The point (ii) of this lemma tells us that for any trajectory of $\Sigma^+_{\theta,k,\gamma,\delta}$ (or $\Sigma^-_{\theta,k,\gamma,\delta}$) crossing a box $B_{a_1a_2a_3}$ with one a_i equal to 1, the time spent in this box is constant: indeed, it does not depend on the initial condition (belonging to the wall $x_i = \theta_i + \delta$ or $x_i = \theta_i - \delta$) of this trajectory.

Proof. [Proof of Lemma 3.8] (i) This first point directly comes from the definition of the exterior and interior systems. For instance in the box B_{222} any trajectory of $\Sigma^+_{\theta,k,\gamma,\delta}$ (or $\Sigma^-_{\theta,k,\gamma,\delta}$) has the following form:

$$\begin{cases} x_1(t) = e^{-\gamma_1 t} x_1(0) \\ x_2(t) = \frac{k_2}{\gamma_2} + e^{-\gamma_2 t}\left(x_2(0) - \frac{k_2}{\gamma_2}\right) \\ x_3(t) = \frac{k_3}{\gamma_3} + e^{-\gamma_3 t}\left(x_3(0) - \frac{k_3}{\gamma_3}\right) \end{cases}.$$

(ii) Let's assume $a_1 = 1$ (this does not restrict the generality). The box B_{122} corresponds to the passing from the wall $x_1 = \theta_1 + \delta$ to the wall $x_1 = \theta_1 - \delta$, while the box B_{100} corresponds

to the reverse direction.
Then, in B_{122} the flows ϕ_t^+ and ϕ_t^- are distinct, but their first components $\left(\phi_t^+\right)_1, \left(\phi_t^-\right)_1$ coincide and are decreasing. Indeed, we have in this box:

$$\begin{aligned} \left(\phi_t^+(x)\right)_1 &= \left(\phi_t^-(x)\right)_1 = e^{-\gamma_1 t} x_1 \\ \frac{k_2}{\gamma_2} + e^{-\gamma_2 t}\left(x_2 - \frac{k_2}{\gamma_2}\right) &= \left(\phi_t^+(x)\right)_2 \geq \left(\phi_t^-(x)\right)_2 = e^{-\gamma_2 t} x_2. \end{aligned}$$

Now let's take x in the switching domain $x_1 = \theta_1 + \delta$. We already know that $\left(\phi_t^-(x)\right)_{t\in\mathbb{R}}$ reaches the wall $x_1 = \theta_1 - \delta$ (as this trajectory follows the cycle $\mathcal{C}$ according to the proof of Lemma 3.5). And as the component $\left(\phi_t^+\right)_2$ is increasing in this box, this is also the case for the trajectory $\left(\phi_t^+(x)\right)_{t\in\mathbb{R}}$. We thus get the hitting time s_1^d (d for "decreasing") from $x_1 = \theta_1 + \delta$ to the wall $x_1 = \theta_1 - \delta$ exists for both ϕ_t^+ and ϕ_t^-, and is equal to:

$$s_1^d = \frac{-1}{\gamma_1} \ln\left(\frac{\theta_1 - \delta}{\theta_1 + \delta}\right).$$

The same reasoning applies to the box B_{100}, for which we have $\left(\phi_t^+(x)\right)_1 = \left(\phi_t^-(x)\right)_1 = \frac{k_1}{\gamma_1} + e^{-\gamma_1 t}\left(x_1 - \frac{k_1}{\gamma_1}\right)$, which leads to a shared hitting time s_1^c (c for "increasing") from $x_1 = \theta_1 - \delta$ to the wall $x_1 = \theta_1 + \delta$ for both of the flows. ■

Now we have:

Lemma 3.9. *Under the assumptions of Lemma 3.5 on the parameters k_i, γ_i, θ_i and δ, the system $\Sigma^+_{\theta,k,\gamma,\delta}$ admits a periodic orbit γ^+.*

Proof. Under the assumptions of Lemma 3.5, there exists a periodic orbit γ^- for $\Sigma^-_{\theta,k,\gamma,\delta}$. We consider the intersection point z^- of γ^- with the wall $\{(x_1, x_2, x_3) \in B_{222} : x_1 = \theta_1 + \delta\}$, and the rectangle $\mathcal{R}$ having z^- as bottom left vertex:

$$\mathcal{R} = \begin{cases} x_1 = \theta_1 + \delta \\ \frac{k_2}{\gamma_2} \geq x_2 \geq {z_2}^- \\ \frac{k_3}{\gamma_3} \geq x_3 \geq {z_3}^- \end{cases}.$$

We are going to track the corresponding inequalities between $\phi_t^-(z^-)$ (that is γ^-) and $\phi_t^+(x)$ in each switching domain: the inequalities obtained step-by-step will permit us to show that $\left(\phi_t^+(x)\right)_{t\in\mathbb{R}}$ also follows the cycle $\mathcal{C}$ and returns to $\mathcal{R}$.
To do this, we need to consider the hitting times at each switching domain. There are two types of such hitting times, corresponding to the two kinds of regular domains (belonging to the cycle $\mathcal{C}$) described by Lemma 3.8. Let's denote by $t_i^{d,-}$, $t_i^{c,-}$ (respectively $t_i^{d,+}$, $t_i^{c,+}$) the times spent by the trajectory γ^- (respectively $\left(\phi_t^+(x)\right)_{t\in\mathbb{R}}$) to cross the boxes $B_{a_1a_2a_3}$ of $\mathcal{C}$ with all $a_i \neq 1$: these hitting times depend on the initial conditions (as said above, the

existence of $t_i^{d,+}$, $t_i^{c,+}$ will be shown step-by-step). In contrast the times s_i^d and s_i^c, given by Lemma 3.8 are independent of the history of the trajectories. The successions of these times "s" and "t" can be represented more clearly in the following way:

$$\begin{array}{ccccccccccc} t_1^{d,*} & & s_1^d & & t_2^{d,*} & & s_2^d & & t_3^{d,*} & & s_3^d \\ B_{222} & \rightarrow & B_{122} & \rightarrow & B_{022} & \rightarrow & B_{012} & \rightarrow & B_{002} & \rightarrow & B_{001} \\ \uparrow & & & & & & & & & & \downarrow \\ B_{221} & \leftarrow & B_{220} & \leftarrow & B_{210} & \leftarrow & B_{200} & \leftarrow & B_{100} & \leftarrow & B_{000} \\ s_3^c & & t_3^{c,*} & & s_2^c & & t_2^{c,*} & & s_1^c & & t_1^{c,*} \end{array} , \tag{3.1}$$

where * denotes the sign + for the trajectory $\left(\phi_t^+(x)\right)_{t\in\mathbb{R}}$ and the sign − for the trajectory γ^-. In this representation, index i refers to the coordinate which is decreasing ("d") or increasing ("c") in the given box. The structure of the proof being based on the succession of these times "s" and "t", it is convenient to gather them two by two by introducing the following notation:

$$\begin{cases} T_1^* &= {t_2}^{d,*} + s_1^d \\ T_2^* &= {t_3}^{d,*} + s_2^d \\ T_3^* &= {t_1}^{c,*} + s_3^d \\ T_4^* &= {t_2}^{c,*} + s_1^c \\ T_5^* &= {t_3}^{c,*} + s_2^c \\ T_6^* &= {t_1}^{d,*} + s_3^c \end{cases} .$$

(i) Let's take a point $x = (x_1, x_2, x_3)$ in $\mathcal{R}$. The trajectories $\left(\phi_t^-(z^-)\right)_{t\in\mathbb{R}}$ and $\left(\phi_t^+(x)\right)_{t\in\mathbb{R}}$ first cross the box B_{122} and, according to Lemma 3.8, reach the wall $x_1 = \theta_1 - \delta$ in the same time s_1^d. The fact they hit the plane $x_1 = \theta_1 - \delta$ at the same time guarantees that the inequalities between x and z^- in $\mathcal{R}$ are preserved in the section $x_1 = \theta_1 - \delta$. More precisely:

$$\begin{aligned} \frac{k_2}{\gamma_2} + e^{-\gamma_2 s_1^d}\left(x_2 - \frac{k_2}{\gamma_2}\right) = \left(\phi_{s_1^d}^+(x)\right)_2 > \left(\phi_{s_1^d}^-(z^-)\right)_2 = e^{-\gamma_2 s_1^d} z_2^- \\ \left(\phi_{s_1^d}^+(x)\right)_3 \geq \left(\phi_{s_1^d}^-(z^-)\right)_3 . \end{aligned}$$

From these inequalities we get that $\left(\phi_t^+(x)\right)_{t\in\mathbb{R}}$ enters the box B_{022}, since γ^- does. According to Lemma 3.8 the expressions of these trajectories are the same in this box. The hitting times of the plane $x_2 = \theta_2 + \delta$ are here given by:

$$t_2^{d,-} = \frac{-1}{\gamma_2} \ln\left(\frac{\theta_2 + \delta}{\left(\phi_{s_1^d}^-(z^-)\right)_2}\right) \tag{3.2}$$

$$t_2^{d,+} = \frac{-1}{\gamma_2} \ln\left(\frac{\theta_2 + \delta}{\left(\phi_{s_1^d}^+(x)\right)_2}\right) \tag{3.3}$$

and thus:

$$t_2^{d,-} < t_2^{d,+}. \tag{3.4}$$

Since the flows ϕ_t^+ and ϕ_t^- coincide in this box we get:

$$\begin{aligned}\left(\phi^+_{T_1^+}(x)\right)_1 &< \left(\phi^-_{T_1^-}(z^-)\right)_1\\ \left(\phi^+_{T_1^+}(x)\right)_3 &> \left(\phi^+_{T_1^-}(x)\right)_3 > \left(\phi^-_{T_1^-}(z^-)\right)_3.\end{aligned}$$

From these inequalities we get by Lemma 3.8 again, that $\left(\phi_t^+(x)\right)_{t\in\mathbb{R}}$ crosses the box B_{012} like the trajectory γ^-.

(ii) Now we repeat the same reasoning in two steps as in (i) for the remaining regular domains, until we reach again the box B_{122}. Let's take the shared time s_2^d at which the two trajectories reach the plane $x_2 = \theta_2 - \delta$. As in (i), we have preservation of the last inequalities obtained in the plane $x_2 = \theta_2 + \delta$, i.e we have:

$$\begin{aligned}\left(\phi^+_{s_2^d+T_1^+}(x)\right)_1 &< \left(\phi^-_{s_2^d+T_1^-}(z^-)\right)_1\\ \left(\phi^+_{s_2^d+T_1^+}(x)\right)_3 &> \left(\phi^-_{s_2^d+T_1^-}(z^-)\right)_3.\end{aligned}$$

Then following the succession of the hitting times described by the graph (3.1) above, it yields:

$$\begin{aligned}\left(\phi^+_{T_2^+ +T_1^+}(x)\right)_1 &< \left(\phi^-_{T_2^- +T_1^-}(z^-)\right)_1\\ \left(\phi^+_{T_2^+ +T_1^+}(x)\right)_2 &< \left(\phi^-_{T_2^- +T_1^-}(z^-)\right)_2,\end{aligned}$$

$$\begin{aligned}\left(\phi^+_{\sum_{i=1}^3 T_i^+}(x)\right)_2 &< \left(\phi^-_{\sum_{i=1}^3 T_i^-}(z^-)\right)_2\\ \left(\phi^+_{\sum_{i=1}^3 T_i^+}(x)\right)_3 &< \left(\phi^-_{\sum_{i=1}^3 T_i-}(z^-)\right)_3,\end{aligned}$$

and:

$$\begin{aligned}\left(\phi^+_{\sum_{i=1}^4 T_i^+}(x)\right)_1 &> \left(\phi^-_{\sum_{i=1}^4 T_i^-}(z^-)\right)_2\\ \left(\phi^+_{\sum_{i=1}^4 T_i^+}(x)\right)_3 &< \left(\phi^-_{\sum_{i=1}^4 T_i^-}(z^-)\right)_3\end{aligned}$$

and then:

$$\begin{aligned}\left(\phi^+_{\sum_{i=1}^5 T_i^+}(x)\right)_1 &> \left(\phi^-_{\sum_{i=1}^5 T_i^-}(z^-)\right)_1\\ \left(\phi^+_{\sum_{i=1}^5 T_i^+}(x)\right)_2 &> \left(\phi^-_{\sum_{i=1}^5 T_i^-}(z^-)\right)_2.\end{aligned}$$

Finally, from this last inequality we get (as before by Lemma 3.8):

$$\left(\phi^{+}_{s_3^c+\sum_{i=1}^{5} T_i^{+}}(x)\right)_1 > \left(\phi^{-}_{s_3^c+\sum_{i=1}^{5} T_i^{-}}\left(z^{-}\right)\right)_1$$
$$\left(\phi^{+}_{s_3^c+\sum_{i=1}^{5} T_i^{+}}(x)\right)_2 > \left(\phi^{-}_{s_3^c+\sum_{i=1}^{5} T_i^{-}}\left(z^{-}\right)\right)_2,$$

where the hitting time of the plane $x_3 = \theta_3 + \delta$ is s_3^c (again according to Lemma 3.8). Thus the trajectory $\left(\phi_t^{+}(x)\right)_{t\in\mathbb{R}}$ crosses the box B_{222} like γ^{-}. Then both of them return to the plane $x_1 = \theta_1 + \delta$ at the times $t_1^{d,+}$ and $t_1^{d,-}$:

$$t_1^{d,-} = \frac{-1}{\gamma_1} \ln\left(\frac{\theta_1+\delta}{\left(\phi^{-}_{s_3^c+\sum_{i=1}^{5} T_i^{-}}\left(z^{-}\right)\right)_1}\right)$$
$$t_1^{d,+} = \frac{-1}{\gamma_1} \ln\left(\frac{\theta_1+\delta}{\left(\phi^{+}_{s_3^c+\sum_{i=1}^{5} T_i^{+}}(x)\right)_1}\right)$$

and thus:

$$t_1^{d,-} < t_1^{d,+},$$

from which we finally get:

$$\left(\phi^{+}_{\sum_{i=1}^{6} T_i^{+}}(x)\right)_2 > \left(\phi^{-}_{\sum_{i=1}^{6} T_i^{-}}\left(z^{-}\right)\right)_2 = z_2^{-}$$
$$\left(\phi^{+}_{\sum_{i=1}^{6} T_i^{+}}(x)\right)_3 > \left(\phi^{-}_{\sum_{i=1}^{6} T_i^{-}}\left(z^{-}\right)\right)_3 = z_3^{-}.$$

In conclusion, $\mathcal{R}$ is a Poincaré section for the flow of $\Sigma^{+}_{\theta,k,\gamma,\delta}$: thus, by the Brouwer fixed point theorem, $\Sigma^{+}_{\theta,k,\gamma,\delta}$ admits a periodic orbit γ^{+} which follows the cycle $\mathcal{C}$ as the periodic orbit γ^{-} does, and which never crosses the cube $\mathcal{C}_\delta$. ■

Remark 3.10. *The existence of the periodic orbit γ^{+} for the exterior system could have been established thanks to a theorem of E. Farcot and J.-L. Gouzé (see [7]), which gives (under assumptions fulfilled by the exterior system) the uniqueness and global stability of the orbit. However, we do not need these additional results for our purpose, and, moreover, our proof of Lemma 3.9 above will be used in the next section for the proof of our main result.*

4. Existence of a Poincaré section for the differential system $\Sigma^{\mu}_{\theta,k,\gamma,\delta}$. We can now prove our main result, which establishes the existence of a periodic orbit for the smooth non monotonic negative feedback circuit $\Sigma^{\mu}_{\theta,k,\gamma,\delta}$, as expected by L. Glass and J. S. Pasternack in [16]:

Theorem 4.1. *Assuming the hypotheses of Lemma 3.5 on the parameters k_i, γ_i, θ_i and δ are satisfied, consider the periodic orbits γ^{-} and γ^{+} of $\Sigma^{-}_{\theta,k,\gamma,\delta}$ and of $\Sigma^{+}_{\theta,k,\gamma,\delta}$ respectively.*

Then the differential system $\Sigma^{\mu}_{\theta,k,\gamma,\delta}$ admits the following rectangle $\mathcal{R}\left(z^{-},z^{+}\right)$ as a Poincaré section:

$$\mathcal{R}\left(z^{-},z^{+}\right)=\begin{cases}x_1=\theta_1+\delta\\ z_2^{+}\geq x_2\geq z_2^{-}\\ z_2^{+}\geq x_3\geq z_3^{-}\end{cases},$$

where z^{-} and z^{+} are the intersection points of γ^{-} and γ^{+} with the plane $x_1=\theta_1+\delta$. In particular, there exists a periodic orbit γ^{μ} for $\Sigma^{\mu}_{\theta,k,\gamma,\delta}$, which follows the cycle $\mathcal{C}$ and which stays outside from the cube $\mathcal{C}_{\delta}$.

Proof. Let's take a point x in the rectangle $\mathcal{R}\left(z^{-},z^{+}\right)$. To establish the theorem, it suffices to re-apply step-by-step the proof of Lemma 3.9, and to verify, using the successive inequalities of this lemma, that for any time t the point $\phi_t^{\mu}\left(x\right)$ belongs to the segment joining $\phi_t^{-}\left(z^{-}\right)$ to ${\phi_t}^{+}\left(z^{+}\right)$.
Throughout the proof, $\mathrm{g}^{-},\mathrm{g}^{\mu},\mathrm{g}^{+}$ denote the three vector fields associated with $\Sigma^{-}_{\theta,k,\gamma,\delta}$, $\Sigma^{\mu}_{\theta,k,\gamma,\delta}$, $\Sigma^{+}_{\theta,k,\gamma,\delta}$.

We first consider again the time s_1^d at which the trajectories γ^{-} and γ^{+} hit the wall $x_1=\theta_1-\delta$ (see Lemma 3.8). We have:

$$\forall t\in[0,s_1^d],\ \left(\phi_t^{-}\left(x\right)\right)_2=x_2e^{-\gamma_2 t}\leq\frac{k_2}{\gamma_2}+e^{-\gamma_2 t}\left(x_2-\frac{k_2}{\gamma_2}\right)=\left(\phi_t^{+}\left(x\right)\right)_2.$$

Since the inequality $\mathrm{g}_2^{-}\leq\mathrm{g}_2^{\mu}\leq\mathrm{g}_2^{+}$ holds in B_{122}, the Gronwall Lemma gives us:

$$\forall t\in[0,s_1^d],\ \left(\phi_t^{-}\left(x\right)\right)_2\leq\left(\phi_t^{\mu}\left(x\right)\right)_2\leq\left(\phi_t^{+}\left(x\right)\right)_2 \tag{4.1}$$

and thus by monotonicity of the flows ${\phi_t}^{-}$ and ${\phi_t}^{+}$ in the box B_{122}, it follows that:

$$\forall t\in[0,s_1^d],\ \left(\phi_t^{-}\left(z^{-}\right)\right)_2\leq\left(\phi_t^{\mu}\left(x\right)\right)_2\leq\left(\phi_t^{+}\left(z^{+}\right)\right)_2. \tag{4.2}$$

By the same reasoning:

$$\forall t\in[0,s_1^d],\ \left(\phi_t^{-}\left(z^{-}\right)\right)_3\leq\left(\phi_t^{\mu}\left(x\right)\right)_3\leq\left(\phi_t^{+}\left(z^{+}\right)\right)_3.$$

Then, as we have $\mathrm{g}^{-}=\mathrm{g}^{\mu}=\mathrm{g}^{+}$ in B_{022} (by Lemma 3.8), the three flows coincide in this box. Thus $\left(\phi_t^{\mu}\left(x\right)\right)_{t\in\mathbb{R}}$ hits the plane $x_2=\theta_2+\delta$ at a time $t_2^{d,\mu}$. According to (4.1) and (3.4), we have:

$$t_2^{d,-}\leq t_2^{d,\mu}\leq t_2^{d,+}$$

and so:

$$\forall t\in[s_1^d,T_1^{-}],\ \left(\phi_t^{+}\left(z^{+}\right)\right)_1=\left(\phi_t^{\mu}\left(x\right)\right)_1=\left(\phi_t^{-}\left(z^{-}\right)\right)_1.$$

But in the box B_{012}, the expression of $\left(\phi_t^-\right)_1$ stays the same, namely we still have: $\phi_t^-(x)_1 = x_1 e^{-\gamma_1 t}$ for every x in B_{012} and for any t such that $\phi_t^-(x)$ stays in this box. From this we get:

$$\forall t \in [s_1^d, T_1^+],\ \left(\phi_t^+\left(z^+\right)\right)_1 = \left(\phi_t^\mu(x)\right)_1 = \left(\phi_t^-\left(z^-\right)\right)_1$$

and:

$$\left(\phi^+_{T_1^+}\left(z^+\right)\right)_1 \leq \left(\phi^\mu_{T_1^\mu}(x)\right)_1 \leq \left(\phi^-_{T_1^-}\left(z^-\right)\right)_1,$$

where we have set $T_1^\mu = t_2^{d,\mu} + s_1^d$. Similarly we get:

$$\forall t \in [s_1^d, T_1^+],\ \left(\phi_t^+\left(z^+\right)\right)_3 \geq \left(\phi_t^\mu(x)\right)_3 \geq \left(\phi_t^-\left(z^-\right)\right)_3$$

and:

$$\left(\phi^+_{T_1^+}\left(z^+\right)\right)_3 \geq \left(\phi^\mu_{T_1^\mu}(x)\right)_3 \geq \left(\phi^-_{T_1^-}\left(z^-\right)\right)_3.$$

Repeating the same argument again, we finally obtained that for any time t and for $i = 1, 2, 3$:

$$\phi_t^\mu(x)_i \in [\phi_t^-\left(z^-\right)_i, \phi_t^+\left(z^+\right)_i] \cup [\phi_t^+\left(z^+\right)_i, \phi_t^-\left(z^-\right)_i]$$

and:

$$\begin{aligned}
\left(\phi^+_{\sum_{i=1}^6 T_i^+}\left(z^+\right)\right)_2 &> \left(\phi^\mu_{\sum_{i=1}^6 T_i^\mu}(x)\right)_2 > \left(\phi^-_{\sum_{i=1}^6 T_i^-}\left(z^-\right)\right)_2 \\
\left(\phi^+_{\sum_{i=1}^6 T_i^+}\left(z^+\right)\right)_3 &> \left(\phi^\mu_{\sum_{i=1}^6 T_i^\mu}(x)\right)_3 > \left(\phi^-_{\sum_{i=1}^6 T_i^-}\left(z^-\right)\right)_3,
\end{aligned}$$

where the times T_i^μ are defined similarly as the times T_i^*. In other words we have:

$$\left(\phi^\mu_{\sum_{i=1}^6 T_i^\mu}(x)\right) \in \mathcal{R}\left(z^-, z^+\right),$$

as desired. As previously, the Brouwer fixed point theorem permits us to conclude there exists a fixed point z^μ of the Poincaré return map in $\mathcal{R}(z^-, z^+)$, and thus a periodic orbit γ^μ for $\Sigma^\mu_{\theta,k,\gamma,\delta}$ passing through z^μ. By construction γ^μ follows the cycle $\mathcal{C}$ and stays outside from $\mathcal{C}_\delta$, like γ^- and γ^+. ■

Remark 4.2. *This theorem is an existence result on periodic oscillations for the continuous model $\Sigma^\mu_{\theta,k,\gamma,\delta}$. It provides neither stability nor uniqueness of our solution γ^μ (even though we can suspect such characteristics for this orbit), and does not exclude other complicated behaviors around this periodic orbit.*

Numerical simulations shown in Section 5 below illustrate this result (see Figure 7 and 8). The size of the Poincaré section $\mathcal{R}(z^-, z^+)$ depends on δ: when δ tends to 0, the two points z^- and z^+ converge to a same point. The periodic orbit γ^μ of the differential system belongs to a rectangular solid torus constructed by γ^- and γ^+: in each plane x_i = constant, the projections of γ^- and γ^+ bound the projection of γ^μ (see 8). In Figure 4, we have represented the area $\mathrm{A}[\mathcal{R}(z^-, z^+)]$ of the section $\mathcal{R}(z^-, z^+)$ as a function of δ, for two sets of parameters θ_i, k_i, γ_i: the two figures suggest this area has a monomial growth (with an exponent proportional to $\min_i \theta_i$) in the parameter δ.

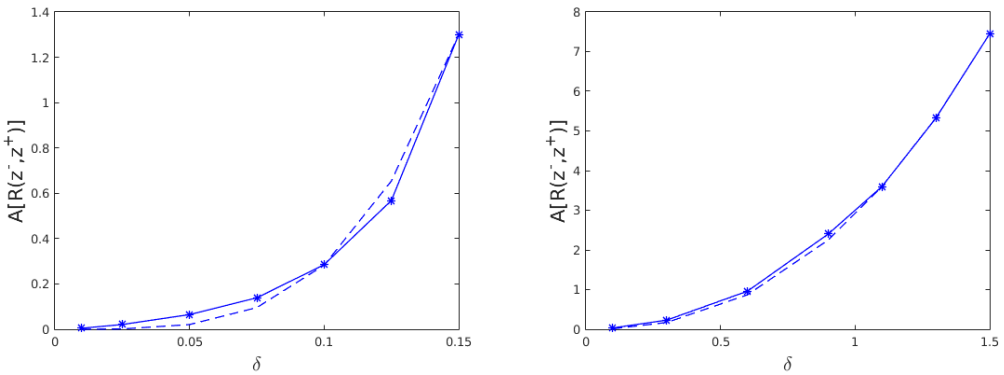

(a) Fitting with the graph (in dots) of the monomial function $2.888\,x^{2.34}$.

(b) Fitting with the graph (in dots) of the monomial function $1639.3\,x^{3.76}$.

Figure 4. *Polynomial growth of the area* $\mathrm{A}[\mathcal{R}\left(z^{-},z^{+}\right)]$ *of* $\mathcal{R}\left(z^{-},z^{+}\right)$ *as a function of* δ. *For the figure on the left, the chosen set of parameters is* $(\theta_i,k_i,\gamma_i)=(2.1,3.3,4.5;\ 3.4,9.0,11.5;\ 0.7,1.3,1.5)$, *for the one on the right it is* $(\theta_i,k_i,\gamma_i)=(16.0,16.3,16.5;\ 1.19,1.19,1.19;\ 0.02,0.02,0.02)$.

5. Applications to synthetic genetic models: the "Repressilator" example. To illustrate this work we now apply our mathematical framework to the well known "Repressilator" system, a biological synthetic circuit designed and implemented by M. B. Elowitz and S. Leibler (see [5]). This network is composed of three genes that repress one another according to a negative feedback loop with three negative arrows (-,-,-). Namely, the protein LacI (encoded by gene *lacI*) inhibits transcription of gene *tetR* which codes for protein TetR and this, in turn, inhibits transcription of a third gene *cI*. Finally Protein CI (encoded by gene *cI*) inhibits expression of gene *lacI*, closing by the way the loop formed by these three proteins (see Figure 5). The three genes were built into a plasmid and inserted in the bacteria *Escherichia coli*. As the bacteria grow, the genes are expressed and the dynamics of the negative circuit can be inferred from the measurements of gene *tetR* expression. The curves reported in [5]

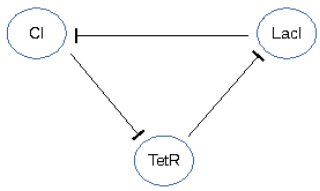

Figure 5. *The interaction graph of the "Repressilator" network, having the form (-,-,-).*

show periodic oscillatory behavior in spite of large intercellular variability. The measurements shown in Figure 2 of [5], are reproduced in blue in Figure 6.

5.1. Equivalence between negative feedback loops (-,-,-) and (-,+,+). To compare our non monotonic negative loop model to the data provided by Figure 6, the first thing to deal with is the form of the negative feedback network: as the reader may have noticed, the systems concerned by our setting are negative circuits of the form (-,+,+), while the "Repressilator" is

of the form (-,-,-). However the two are equivalent under a simple change of variables. Indeed, consider a piecewise linear negative feedback network (-,-,-):

$$\begin{cases} \dot{x_1} &= k_1 s^- (x_3, \theta_3, \delta) - \gamma_1 x_1 \\ \dot{x_2} &= k_2 s^- (x_1, \theta_1, \delta) - \gamma_2 x_2 \\ \dot{x_3} &= k_3 s^- (x_2, \theta_2, \delta) - \gamma_3 x_3 \end{cases},$$

and set:

$$w_2 = \frac{k_2}{\gamma_2} - x_2, \ w_1 = x_1, \ w_3 = x_3.$$

With this change of variables it follows that:

$$\begin{cases} \dot{w_1} &= k_1 s^- (w_3, \theta_3, \delta) - \gamma_1 w_1 \\ \dot{w_2} &= k_2 s^+ (w_1, \theta_1, \delta) - \gamma_2 w_2 \\ \dot{w_3} &= k_3 s^- \left(\frac{k_2}{\gamma_2} - w_2, \theta_2, \delta \right) - \gamma_3 w_3 \end{cases},$$

where we have used the relation $k_2 - k_2 s^- (w_1, \theta_1, \delta) = k_2 s^+ (w_1, \theta_1, \delta)$ in equation $\dot{w_2}$. Observing the following relation:

$$s^- \left(\frac{k_2}{\gamma_2} - w_2, \theta_2, \delta \right) = \begin{cases} 1, \text{ if } w_2 > \frac{k_2}{\gamma_2} - \theta_2, \\ \\ 0, \text{ if } w_2 < \frac{k_2}{\gamma_2} - \theta_2, \end{cases} \equiv s^+ \left(w_2, \tilde{\theta}_2 \right),$$

where $\tilde{\theta}_2$ is defined by $\tilde{\theta}_2 = \frac{k_2}{\gamma_2} - \theta_2$, we thus have now a negative feedback circuit of the form (-,+,+), with new thresholds $(\theta_1, \tilde{\theta}_2, \theta_3)$. The same reasoning applies to smooth negative feedback circuits, where s^-, s^+ are replaced by smooth functions μ^-, μ^+.

5.2. Application to the "Repressilator" data. As said in Subsection 5.1, while the bacteria grow and divide, the expression of one gene is tracked thanks to a reporter gene. The data of Figure 6 consists of 60 fluorescence points, $\tilde{a}(t_j) : j = 1, ..., 60$, taken at regular 10 minutes intervals ($t_1 = 10, t_i + 1 = t_i + 10$), representing this gene expression. The points show a marked oscillatory dynamics with four peaks but the period is noisy and superimposed with an increasing linear trend. As it was done in [34], we can correct the data for this trend, for instance by letting:

$$a(t_j) = \tilde{a}(t_j) - \frac{1}{15} t_j.$$

it is possible to obtain a period, T_d, and peak amplitude M_d, from the first (corrected) 40 points, which correspond to two periods. We look for a model $\Sigma^{\mu}_{\theta,k,\gamma,\delta}$ with $\gamma_i = \gamma$

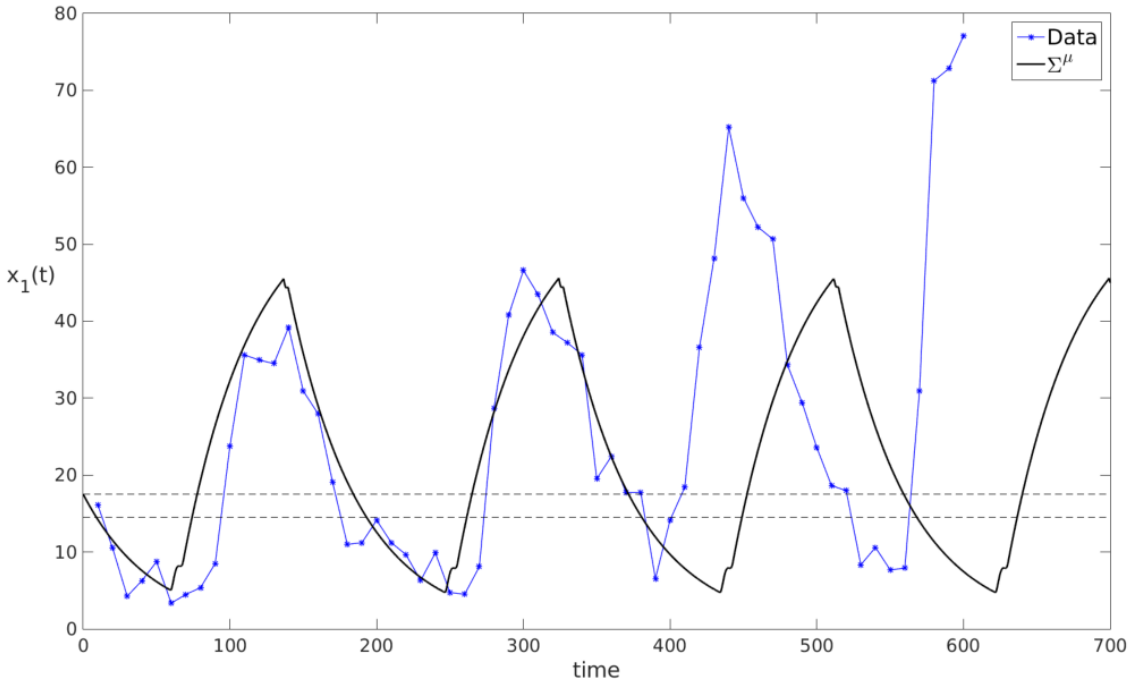

Figure 6. *Comparing (corrected) "Repressilator" data (blue dots) and variable x_1 of model $\Sigma^{\mu}_{\theta,k,\gamma,\delta}$ (black curve) with non-monotone μ. Estimated parameters: $\theta_1 = 16.0$, $\theta_2 = 16.3$, $\theta_3 = 16.5$, $\delta = 1.5$, $\gamma_i = 0.02$, and $k_i = 1.19$.*

and $k_i = k$ for all i (for simplicity). More precisely, fixing first the form of μ, we search for a parameter vector ${p_\mu}^* = (k, \gamma, \delta, \theta_1, \theta_2, \theta_3)$ that minimizes the cost function $\mathrm{J}\left({p_\mu}^*\right) = \min_p[(\mathrm{T}_\mu\left(p_\mu\right) - \mathrm{T}_d)^2 + (\mathrm{M}_\mu\left(p_\mu\right) - \mathrm{M}_d)^2]$. Different forms of μ were tested (linear, quadratic, and cubic) and in each case a parameter vector ${p_\mu}^*$ was estimated. With the following choice of the function μ^0 (represented in Figure 2):

$$\mu^0\left(x, \theta, \delta\right) = \begin{cases} 0, \text{ if } x \leq \theta - \delta \\ c_3 x^3 + c_2 x^2 + c_1 x + c_0, \text{ if } \theta - \delta \leq x \leq \theta + \delta \\ 1, \text{ if } x \geq \theta + \delta \end{cases},$$

where the coefficients c_j are computed from continuity constraints and the following conditions:

$$\begin{cases} \mu\left(\theta - \dfrac{\delta}{2}\right) = 0.9 \\ \mu\left(\theta + \dfrac{\delta}{2}\right) = 0.1 \end{cases},$$

we obtain the result shown in Figure 6 (the optimization was performed by Matlab). The model $\Sigma^{\mu^0}_{\theta,k,\gamma,\delta}$ reproduces several quantities of the data points, such as the period and the maximal and minimal amplitudes of the oscillations. The area of the Poincaré section is

approximately 1 for $\delta = 0.6$ and 7.5 for $\delta = 1.5$ (see Figure 7). For $\delta \geq 1.5$ the periodic orbit γ^- crosses the middle cube $\mathcal{C}_\delta$ (in blue) and hence our theorem does not apply for large δ. The fact that different forms of μ can explain the data equally well indicates that our framework is suitable to describe systems with high variability and noise (as often happens in biological networks). For instance, the flexibility in choosing μ may help reproducing particular details, such as local variations near the maxima and minima, as in Figure 6. Another interesting property of this framework is the possibility of detecting an unknown interval, of width 2δ, independently of the form of μ. In this example, for the different forms of μ, the estimate is $\delta \in [0.5, 1.5]$, for θ_i around 10. Further measurements, namely the expression of a second gene, would lead to more accurate estimates of δ.

6. Generalization to higher dimensions. The result given by Theorem 4.1 can be easily extended to dimension $n \geq 3$. In this case our model $\Sigma^{\mu}_{\theta,k,\gamma,\delta}$ has the following form:

$$\Sigma^{\mu}_{\theta,k,\gamma,\delta}: \begin{cases} \dot{x_1} &= k_1\mu^-\left(x_n,\theta_n,\delta\right) - \gamma_1 x_1 \\ \dot{x_2} &= k_2\mu^+\left(x_1,\theta_1,\delta\right) - \gamma_2 x_2 \\ \vdots & \\ \dot{x_i} &= k_i\mu^+\left(x_{i-1},\theta_{i-1},\delta\right) - \gamma_i x_i \\ \vdots & \\ \dot{x_n} &= k_n\mu^+\left(x_{n-1},\theta_{n-1},\delta\right) - \gamma_n x_n \end{cases}.$$

The exterior piecewise linear system $\Sigma^{+}_{\theta,k,\gamma,\delta}$ becomes:

$$\begin{cases} x_1(t) = k_1\left(s^-\left(x_n,\theta_n+\delta\right)s^+\left(x_1,\theta_1+\delta\right) + s^-\left(x_n,\theta_n-\delta\right)s^-\left(x_1,\theta_1+\delta\right)\right) - \gamma_1 x_1 \\ x_2(t) = k_2\left(s^+\left(x_1,\theta_1+\delta\right)s^-\left(x_2,\theta_2+\delta\right) + s^+\left(x_1,\theta_1-\delta\right)s^+\left(x_2,\theta_2+\delta\right)\right) - \gamma_2 x_2 \\ \vdots \\ x_i(t) = k_i\left(s^+\left(x_{i-1},\theta_{i-1}+\delta\right)s^-\left(x_i,\theta_i+\delta\right) + s^+\left(x_{i-1},\theta_{i-1}-\delta\right)s^+\left(x_i,\theta_i+\delta\right)\right) - \gamma_i x_i \\ \vdots \\ x_n(t) = k_n\left(s^+\left(x_{n-1},\theta_{n-1}+\delta\right)s^-\left(x_n,\theta_n+\delta\right) + s^+\left(x_{n-1},\theta_{n-1}-\delta\right)s^+\left(x_n,\theta_n+\delta\right)\right) - \gamma_n x_n \end{cases}$$

and the interior $\Sigma^{-}_{\theta,k,\gamma,\delta}$ is:

$$\begin{cases} x_1(t) = k_1\left(s^-\left(x_n,\theta_n-\delta\right)s^+\left(x_1,\theta_1+\delta\right) + s^-\left(x_n,\theta_n+\delta\right)s^-\left(x_1,\theta_1+\delta\right)\right) - \gamma_1 x_1 \\ x_2(t) = k_2\left(s^+\left(x_1,\theta_1-\delta\right)s^-\left(x_2,\theta_2+\delta\right) + s^+\left(x_1,\theta_1+\delta\right)s^+\left(x_2,\theta_2+\delta\right)\right) - \gamma_2 x_2 \\ \vdots \\ x_i(t) = k_i\left(s^+\left(x_{i-1},\theta_{i-1}-\delta\right)s^-\left(x_i,\theta_i+\delta\right) + s^+\left(x_{i-1},\theta_{i-1}+\delta\right)s^+\left(x_i,\theta_i+\delta\right)\right) - \gamma_i x_i \\ \vdots \\ x_n(t) = k_n\left(s^+\left(x_{n-1},\theta_{n-1}-\delta\right)s^-\left(x_n,\theta_n+\delta\right) + s^+\left(x_{n-1},\theta_{n-1}+\delta\right)s^+\left(x_n,\theta_n+\delta\right)\right) - \gamma_n x_n \end{cases}.$$

We now have 3^n regular domains instead of 3^3. Under similar assumptions as in Lemma 3.5 we prove that the interior system $\Sigma^{-}_{\theta,k,\gamma,\delta}$ has a periodic orbit γ^- by showing it admits the

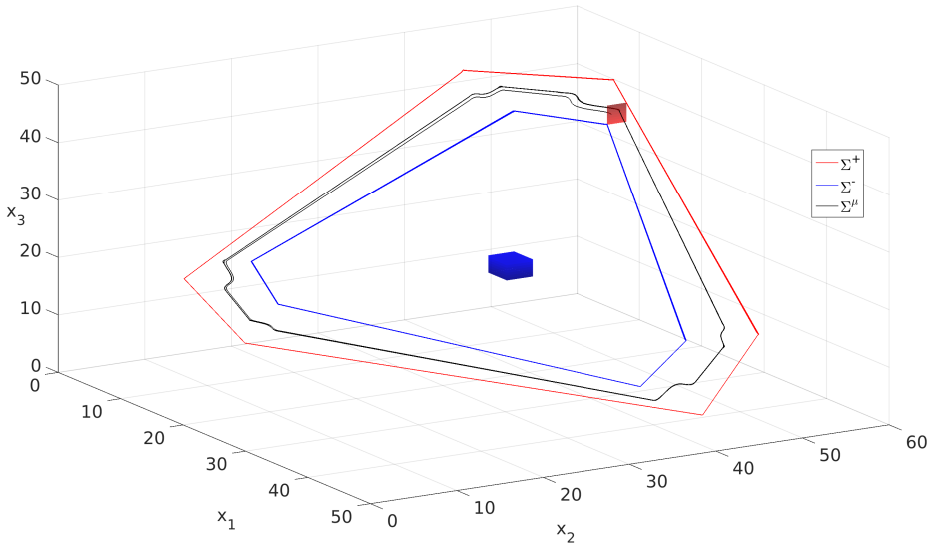

(a) $\delta = 1.5$

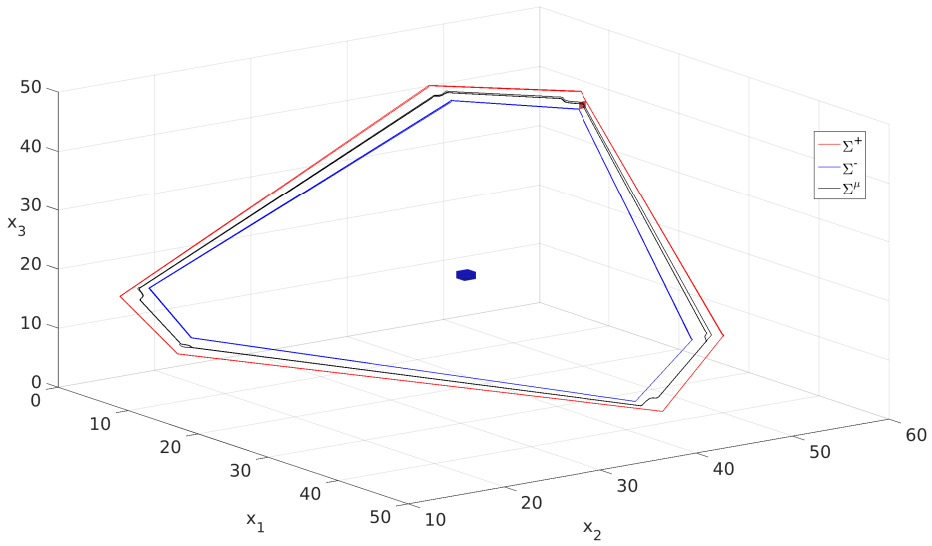

(b) $\delta = 0.6$

Figure 7. *Periodic orbit* γ^{μ^0} *for the non monotonic negative feedback loop* $\Sigma^{\mu^0}_{\theta,k,\gamma,\delta}$ *fitting the "Repressilator" data given by Figure 6, for two values of* δ*. The size of the Poincaré section* $\mathcal{R}\left(z^-, z^+\right)$ *in violet decreases with* δ*. The trajectory* γ^{μ^0} *in black is bounded by the exterior periodic orbit* γ^+ *in red and by the interior one* γ^- *in blue. When* δ *tends to* 0*, the three trajectories collapse to the same orbit. The cube* $\mathcal{C}_\delta$ *is drawn in blue at the center of the figure. Estimated parameters* $\theta_1 = 16.0$*,* $\theta_2 = 16.3$*,* $\theta_3 = 16.5$*,* $\delta = 1.5$*,* $\gamma_i = 0.02$*, and* $k_i = 1.19$*.*

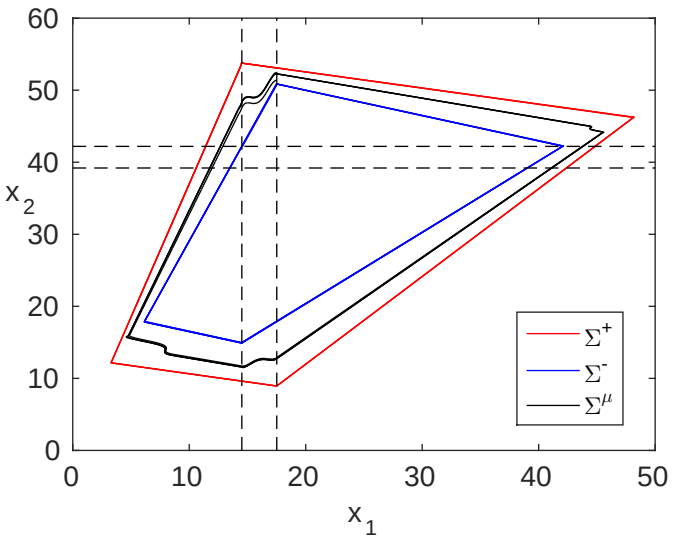

Figure 8. *Projection of the three periodic orbits γ^{μ^0} (in black), γ^+ (in red) and γ^- (in blue) of the previous Figure 7, in the plane x_1, x_2, for the value of parameter $\delta = 1.5$.*

following closed set:

$$(\mathcal{P}): \begin{cases} \dfrac{k_1}{\gamma_1} & \geq x_1 \geq \theta_1 + \eta \\ \dfrac{k_2}{\gamma_2} & \geq x_2 \geq \theta_2 + \delta \\ \vdots & \\ \dfrac{k_i}{\gamma_i} & \geq x_i \geq \theta_i + \delta \\ \vdots & \\ \dfrac{k_{n-1}}{\gamma_{n-1}} & \geq x_{n-1} \geq \theta_{n-1} + \delta \\ x_n & = \theta_n - \delta \end{cases}$$

as a Poincaré section.

The proof of the extended Lemma 3.5 proceeds similarly as before, since the expressions of the flow do not change for dimension $n \geq 3$. The periodic orbit γ^- follows the cycle $\mathcal{C}$ given by:

$$\mathcal{C}: \quad \begin{array}{ccccccccccccc} B_{222\cdots2} & \to & B_{122\cdots2} & \to & B_{022\cdots2} & \to & B_{012\cdots2} & \to & B_{002\cdots2} & \to & \cdots & \to & B_{000\cdots0} \\ \uparrow & & & & & & & & & & & & \downarrow \\ B_{222\cdots1} & \leftarrow & \cdots & \leftarrow & B_{2210\cdots0} & \leftarrow & B_{220\cdots0} & \leftarrow & B_{210\cdots0} & \leftarrow & B_{200\cdots0} & \leftarrow & B_{100\cdots0} \end{array}$$

while staying away from the cube $\mathcal{C}_\delta = [\theta_1 - \delta, \theta_1 + \delta] \times \cdots \times [\theta_n - \delta, \theta_n + \delta]$ around the threshold $(\theta_1, \cdots, \theta_n)$. Then we prove as in Lemma 3.9 that the exterior system $\Sigma^+_{\theta,k,\gamma,\delta}$ admits a periodic orbit γ^+ by showing the following closed set:

$$\mathcal{R} = \begin{cases} x_1 = \theta_1 + \delta \\ \dfrac{k_2}{\gamma_2} \geq x_2 \geq {z_2}^- \\ \vdots \\ \dfrac{k_i}{\gamma_i} \geq x_i \geq {z_i}^- \\ \vdots \\ \dfrac{k_n}{\gamma_n} \geq x_n \geq {z_n}^- \end{cases}$$

is a Poincaré section (where z^- denotes the intersection point of γ^- with the switching domain $\{(x_1, x_2, x_3, \cdots, x_n) \in B_{222\cdots2} : x_1 = \theta_1 + \delta\}$, as in the proof of Lemma 3.9). From this we get, by exactly the same reasoning as before, the following corollary which is the analog of our main result (given by Theorem 4.1) for $n \geq 3$:

Corollary 6.1. *Given a real number $\eta > 0$, assume the following hypotheses on the parameters $(k_i, \gamma_i, \theta_i)_{1 \leq i \leq n}$ and δ are satisfied: for every $1 \leq i \leq n$, $\theta_i > 0$ and for every $2 \leq i \leq n$, $\dfrac{k_i}{\gamma_i} > \theta_i + \eta$. Then, there exists a real number $\Lambda_0 > \eta$ and a number δ_0 satisfying $0 < \delta_0 < \min_{1 \leq i \leq n} \left(\theta_i, \dfrac{k_i}{\gamma_i} - \theta_i, 1 \right)$ such that for every $\dfrac{k_1}{\gamma_1} > \Lambda_0 + \theta_1$ and every $0 < \delta \leq \delta_0$, the continuous system $\Sigma^\mu_{\theta,k,\gamma,\delta}$ admits a periodic orbit γ^μ.*

7. Conclusion. This paper studies the periodic behavior of a class of negative feedback systems, Σ^μ, where the functions that represent the system's interactions are smooth but may have a (small) window of unknown, nonlinear, non monotonic form. Negative feedback circuits are common in biological systems and are typically associated with oscillatory behavior and biological rhythms. The non monotonicity interval introduced in our approach for the interaction functions allows greater flexibility and more accurate modeling of experimental data, as illustrated by comparison to the "Repressilator" network. Our main contribution is to establish the existence of *an invariant toroidal region for the trajectories of* Σ^μ and, in particular, to show existence of sustained oscillations (and a periodic orbit) for this general class of negative feedback systems. Our method constructs two piecewise linear systems that provide interior and exterior bounds for Σ^μ, each admitting a periodic orbit which, taken together, define the invariant toroidal region. Numerical simulations suggested that the area of any section of this torus has a monomial growth in δ. The method applies for n-dimensional

circuits but we believe it can also be applied to other network motifs, provided the transition diagram of the associated piecewise linear systems contains a "long" cycle of the form $\mathcal{C}$ and under certain conditions on the parameters (this is a work in progress). Another direction for future study is a deeper analysis of the Poincaré section and invariant region: indeed, we strongly suspect the invariant torus is unique, from which we could establish *uniqueness and stability properties* of the periodic orbit of the system Σ^{μ} under additional hypotheses. Further on-going work concerns the analysis of the relationship between the size 2δ of the non-monotonicity window and the area of the Poincaré section. It is clear that the latter increases with δ (see Figure 4), but the form depends on the other parameters, notably on the thresholds θ_i. A deeper analysis of this dependence will lead to better fitting and understanding of the mathematical models with respect to the variability in biological data (see Figure 6).

Appendix: Proof of Lemma 3.5. Here we prove Lemma 3.5 which gives the existence of a periodic orbit for the interior system $\Sigma^{-}_{\theta,k,\gamma,\delta}$.

Proof. [Proof of Lemma 3.5] The idea is to approximate in each box the area of the walls hit by the trajectories of $\Sigma^{-}_{\theta,k,\gamma,\delta}$ starting in $(\mathcal{P})$.

(i) We naturally start in the closed set $(\mathcal{P})$, in which we have to show the trajectories return: let's take an initial condition (x_1, x_2, x_3) in $(\mathcal{P})$.
By definition of $\Sigma^{-}_{\theta,k,\gamma,\delta}$, the trajectory of this system having (x_1, x_2, x_3) as initial condition is:

$$\begin{cases} x_1(t) = e^{-\gamma_1 t} x_1 \\ x_2(t) = \dfrac{k_2}{\gamma_2} + e^{-\gamma_2 t}\left(x_2 - \dfrac{k_2}{\gamma_2}\right) \\ x_3(t) = \dfrac{k_3}{\gamma_3} + e^{-\gamma_3 t}\left(x_3 - \dfrac{k_3}{\gamma_3}\right) \end{cases}.$$

The first coordinate $x_1(t)$ is decreasing as t increases: so there exists a time $t_1 > 0$ such that $x_1(t_1) - \theta_1 = \delta$ (at which time the expression of the flow changes), and more precisely we have: $t_1 = \dfrac{-1}{\gamma_1} \ln\left(\dfrac{\theta_1 + \delta}{x_1}\right)$. Replacing in the expressions of $x_2(t)$, it comes:

$$\begin{aligned} x_2(t_1) - \theta_2 &\geq \left(\frac{k_2}{\gamma_2} - \theta_2\right)\left(1 - \left(\frac{\theta_1 + \delta}{x_1}\right)^{\frac{\gamma_2}{\gamma_1}}\right) + \delta\left(\frac{\theta_1 + \delta}{x_1}\right)^{\frac{\gamma_2}{\gamma_1}} \\ &> \left(\frac{k_2}{\gamma_2} - \theta_2\right)\left(1 - \left(\frac{\theta_1 + \delta}{\theta_1 + \eta}\right)^{\frac{\gamma_2}{\gamma_1}}\right) \\ &> \delta \end{aligned}$$

for a choice of $\delta > 0$ small enough, that is to say for $0 < \delta < \delta_1$ where $0 < \delta_1 < \dfrac{k_2}{\gamma_2} - \theta_2$ is

chosen small enough (such a real number δ_1 exists by continuity). Similarly we have:

$$x_3(t_1) - \theta_3 > \left(\frac{k_3}{\gamma_3} - \theta_3\right) - \left(\frac{\theta_1 + \delta}{\theta_1 + \eta}\right)^{\frac{\gamma_3}{\gamma_1}} \left(\frac{k_3}{\gamma_3} - \theta_3 + \delta\right)$$

and by continuity in δ this last expression is strictly greater than δ for δ satisfying $0 < \delta < \delta_1'$, where $0 < \delta_1' < \dfrac{k_3}{\gamma_3} - \theta_3$ is chosen small enough. Notice that in t_1 we have reached the box B_{122}, after having crossed the box B_{222}.

(ii) Then let's take an initial condition (x_1, x_2, x_3) in the same area as the last point $(x_1(t_1), x_2(t_1), x_3(t_1))$ above, i.e such that:

$$\begin{cases} x_1 - \theta_1 & = \delta \\ x_2 - \theta_2 & > \left(\dfrac{k_2}{\gamma_2} - \theta_2\right)\left(1 - \left(\dfrac{\theta_1 + \delta}{\theta_1 + \eta}\right)^{\frac{\gamma_2}{\gamma_1}}\right) \\ x_3 - \theta_3 & > \left(\dfrac{k_3}{\gamma_3} - \theta_3\right) - \left(\dfrac{\theta_1 + \delta}{\theta_1 + \eta}\right)^{\frac{\gamma_3}{\gamma_1}} \left(\dfrac{k_3}{\gamma_3} - \theta_3 + \delta\right) \end{cases},$$

where δ satisfies $0 < \delta < \min(\delta_1, \delta_1')$. This time, the trajectory starting in (x_1, x_2, x_3) is:

$$\begin{cases} x_1(t) = e^{-\gamma_1 t} x_1 \\ x_2(t) = e^{-\gamma_2 t} x_2 \\ x_3(t) = \dfrac{k_3}{\gamma_3} + e^{-\gamma_3 t}\left(x_3 - \dfrac{k_3}{\gamma_3}\right) \end{cases}.$$

Let $t_2 > 0$ the time for which $x_2(t_2) - \theta_2 = \delta$, i.e $t_2 = \dfrac{-1}{\gamma_2} \ln\left(\dfrac{\theta_2 + \delta}{x_2}\right)$. Then, replacing in the expression of $x_1(t)$, we have:

$$\begin{aligned} x_1(t_2) - \theta_1 &< (\theta_1 + \delta)\left(\frac{\theta_2 + \delta}{x_2}\right)^{\frac{\gamma_1}{\gamma_2}} - \theta_1 \\ &< (\theta_1 + \delta)\left(\frac{\theta_2 + \delta}{\theta_2 + \left(\dfrac{k_2}{\gamma_2} - \theta_2\right)\left(1 - \left(\dfrac{\theta_1 + \delta}{\theta_1 + \eta}\right)^{\frac{\gamma_2}{\gamma_1}}\right)}\right)^{\frac{\gamma_1}{\gamma_2}} - \theta_1, \end{aligned}$$

and again by continuity in δ there exists a real number $0 < \delta_2 < \theta_1$ such that for every $0 < \delta < \delta_2$ this last expression is strictly smaller than $-\delta$. Similarly we have:

$$\begin{aligned} x_3(t_2) - \theta_3 &> \left(\frac{k_3}{\gamma_3} - \theta_3\right) + e^{-\gamma_3 t}\left(x_3 - \frac{k_3}{\gamma_3}\right) \\ &> \left(\frac{k_3}{\gamma_3} - \theta_3\right)\left(1 - \left(\frac{\theta_1+\delta}{\theta_1+\eta}\right)^{\frac{\gamma_3}{\gamma_1}}\right) - \delta \\ &> \delta \end{aligned}$$

for δ satisfying $0 < \delta < \delta_2'$, where $0 < \delta_2'$ is chosen small enough. We have reached B_{012} after having crossed B_{122} and B_{022}.

(iii) Let's now take a value δ verifying $0 < \delta < \min_{i=1,2}(\delta_i, \delta_i')$, and an initial condition (x_1, x_2, x_3) satisfying the last inequalities above, i.e verifying:

$$\begin{cases} x_1 - \theta_1 & < (\theta_1+\delta)\left(\dfrac{\theta_2+\delta}{\theta_2 + \left(\frac{k_2}{\gamma_2} - \theta_2\right)\left(1 - \left(\frac{\theta_1+\delta}{\theta_1+\eta}\right)^{\frac{\gamma_2}{\gamma_1}}\right)}\right)^{\frac{\gamma_1}{\gamma_2}} - \theta_1 \,(< -\delta) \\ x_2 - \theta_2 & = \delta \\ x_3 - \theta_3 & > \left(\frac{k_3}{\gamma_3} - \theta_3\right)\left(1 - \left(\frac{\theta_1+\delta}{\theta_1+\eta}\right)^{\frac{\gamma_3}{\gamma_1}}\right) - \delta \,(> \delta) \end{cases}.$$

Then the orbit starting at (x_1, x_2, x_3) has the form:

$$\begin{cases} x_1(t) = e^{-\gamma_1 t} x_1 \\ x_2(t) = e^{-\gamma_2 t} x_2 \\ x_3(t) = e^{-\gamma_3 t} x_3 \end{cases}.$$

Let $t_3 = \dfrac{-1}{\gamma_3} \ln\left(\dfrac{\theta_3+\delta}{x_3}\right)$ the time at which we have $x_3(t_3) - \theta_3 = \delta$ (i.e the time at which the trajectory hits the hyperplane $x_3 - \theta_3 = \delta$). Replacing in the expression of x_2 we have:

$$x_2(t_3) - \theta_2 < (\theta_2+\delta)\, \mathrm{f}_{\theta_3}(\delta)^{\frac{\gamma_2}{\gamma_3}} - \theta_2$$

where we have set:

$$\mathrm{f}_{\theta_3}(\delta) = \frac{\theta_3 + \delta}{\theta_3 + \left(\dfrac{k_3}{\gamma_3} - \theta_3\right)\left(1 - \left(\dfrac{\theta_1 + \delta}{\theta_1 + \eta}\right)^{\dfrac{\gamma_3}{\gamma_1}}\right) - \delta}.$$

The function f_{θ_3} is increasing in δ and (by continuity again) there exists a real number $0 < \delta_3 < \theta_2$ such that for every $0 < \delta < \delta_3$ we have:

$$(\theta_2 + \delta)\,\mathrm{f}_{\theta_3}(\delta)^{\dfrac{\gamma_2}{\gamma_3}} - \theta_2 < -\delta.$$

Similarly, using the choice of the initial condition x_1 and replacing in the expression of $x_1(t_3)$ we have, for every $0 < \delta < \delta_3$:

$$\begin{aligned} x_1(t_3) - \theta_1 &< (\theta_1 - \delta)\,\mathrm{f}_{\theta_3}(\delta)^{\dfrac{\gamma_1}{\gamma_3}} - \theta_1 \\ &< -\delta. \end{aligned}$$

We have crossed the boxes B_{012} and B_{002} to reach B_{001}.

(iv) Let's go on by taking a value $0 < \delta < \min_{i=1,2}(\delta_i, \delta_i', \delta_3,)$ and an initial condition (x_1, x_2, x_3) verifying:

$$\begin{cases} x_1 - \theta_1 & < (\theta_1 - \delta)\,\mathrm{f}_{\theta_3}(\delta)^{\dfrac{\gamma_1}{\gamma_3}} - \theta_1 \,(< -\delta) \\ x_2 - \theta_2 & < (\theta_2 + \delta)\,\mathrm{f}_{\theta_3}(\delta)^{\dfrac{\gamma_2}{\gamma_3}} - \theta_2 \,(< -\delta) \\ x_3 - \theta_3 & = \delta \end{cases}.$$

The trajectory starting in (x_1, x_2, x_3) has the form:

$$\begin{cases} x_1(t) = \dfrac{k_1}{\gamma_1} + e^{-\gamma_1 t}\left(x_1 - \dfrac{k_1}{\gamma_1}\right) \\ x_2(t) = e^{-\gamma_2 t} x_2 \\ x_3(t) = e^{-\gamma_3 t} x_3 \end{cases}.$$

Let t_4 be the time at which we have $x_1(t_4) - \theta_1 = -\delta$, that is: $t_4 = \dfrac{-1}{\gamma_1} \ln\left(\dfrac{\dfrac{k_1}{\gamma_1} - \theta_1 + \delta}{\dfrac{k_1}{\gamma_1} - x_1}\right)$.

As the component $x_2(t)$ is decreasing in t we have:

$$x_2(t_4) - \theta_2 < (\theta_2 + \delta)\,\mathrm{f}_{\theta_3}(\delta)^{\dfrac{\gamma_2}{\gamma_3}} - \theta_2 < -\delta,$$

by choice of the initial condition (x_1, x_2, x_3). There exists (by the same continuity argument as above) a real $0 < \delta_4 < \min(\theta_3, 1)$ such that for every $0 < \delta < \delta_4$ the following holds:

$$\begin{aligned} x_3(t_4) - \theta_3 &< (\theta_3 + \delta) \left(\frac{\frac{k_1}{\gamma_1} - \theta_1 + \delta}{\frac{k_1}{\gamma_1} - (\theta_1 - \delta) \mathrm{f}_{\theta_3}(\delta)^{\frac{\gamma_1}{\gamma_3}}} \right)^{\frac{\gamma_3}{\gamma_1}} - \theta_3 \\ &< -\delta. \end{aligned}$$

We have crossed the boxes B_{001} and B_{000} to reach the box B_{100}.

(v) Now let us take a value $0 < \delta \leq \min_{i=1,2}(\delta_i, \delta_i', \delta_3, \delta_4)$ and an initial condition (x_1, x_2, x_3) verifying:

$$\begin{cases} x_1 - \theta_1 & = -\delta \\ x_2 - \theta_2 & < (\theta_2 + \delta) \mathrm{f}_{\theta_3}(\delta)^{\frac{\gamma_2}{\gamma_3}} - \theta_2 \, (< -\delta) \\ x_3 - \theta_3 & < (\theta_3 + \delta) \left(\frac{\frac{k_1}{\gamma_1} - \theta_1 + \delta}{\frac{k_1}{\gamma_1} - (\theta_1 - \delta) \mathrm{f}_{\theta_3}(\delta)^{\frac{\gamma_1}{\gamma_3}}} \right)^{\frac{\gamma_3}{\gamma_1}} - \theta_3 \, (< -\delta) \end{cases}.$$

This time the trajectory starting at (x_1, x_2, x_3) is:

$$\begin{cases} x_1(t) = \frac{k_1}{\gamma_1} + e^{-\gamma_1 t}(x_1 - \frac{k_1}{\gamma_1}) \\ x_2(t) = \frac{k_2}{\gamma_2} + e^{-\gamma_2 t}(x_2 - \frac{k_2}{\gamma_2}) \\ x_3(t) = e^{-\gamma_3 t} x_3 \end{cases}.$$

Denote by $t_5 = \frac{-1}{\gamma_2} \ln \left(\frac{\frac{k_2}{\gamma_2} - \theta_2 + \delta}{\frac{k_2}{\gamma_2} - x_2} \right)$ the time at which the trajectory hits the hyperplane $x_2 - \theta_2 = -\delta$, i.e such that: $x_2(t_5) - \theta_2 = -\delta$.

It comes:

$$x_1(t_5) - \theta_1 > \frac{k_1}{\gamma_1} - \theta_1 - \left(\frac{\frac{k_2}{\gamma_2} - \theta_2 + \delta}{\frac{k_2}{\gamma_2} - (\theta_2 + \delta)\, \mathrm{f}_{\theta_3}(\delta)^{\frac{\gamma_2}{\gamma_3}}} \right)^{\frac{\gamma_1}{\gamma_2}} \left(\frac{k_1}{\gamma_1} - \theta_1 + \delta \right).$$

To simplify the notations, let's denote by $\mathrm{g}(\delta)$ the quotient above:

$$\mathrm{g}(\delta) := \frac{\frac{k_2}{\gamma_2} - \theta_2 + \delta}{\frac{k_2}{\gamma_2} - (\theta_2 + \delta)\, \mathrm{f}_{\theta_3}(\delta)^{\frac{\gamma_2}{\gamma_3}}}.$$

The function g is increasing in δ since f_{θ_3} is an increasing function, and for every $0 < \delta \leq \min_{i=1,2}(\delta_i, \delta_i', \delta_3, \delta_4)$ we have $\mathrm{g}(\delta) < 1$.

Now, let's impose $\frac{k_1}{\gamma_1}$ to be great by requiring $\frac{k_1}{\gamma_1} > \Lambda_0 + \theta_1$, where Λ_0 is defined by:

$$\Lambda_0 = \frac{(\eta + 1)}{1 - \mathrm{g}(\delta_0)^{\frac{\gamma_1}{\gamma_2}}}.$$

With such a choice of $\frac{k_1}{\gamma_1}$ we notice the following inequality:

$$\frac{k_1}{\gamma_1} - \theta_1 > \Lambda_0 > \eta + 1 > \delta,$$

(since we have chosen $\delta_4 < 1$) and we have:

$$\begin{aligned} x_1(t_5) - \theta_1 &> \eta + 1 - \delta \\ &> \eta. \end{aligned}$$

And as x_3 is decreasing in t we have, by choice of the initial condition x_3:

$$\begin{aligned} x_3(t_5) - \theta_3 &< (\theta_3 - \delta)\, \mathrm{g}(\delta)^{\frac{\gamma_3}{\gamma_2}} - \theta_3 \\ &< -\delta. \end{aligned}$$

We have crossed the boxes B_{100} and B_{200} to reach B_{210}.

(vi) Finally let's take a value $0 < \delta < \min_{i=1,2}(\delta_i, \delta_i', \delta_3, \delta_4)$ and an initial condition satisfying the last inequalities of the previous step, that is to say such that:

$$\begin{cases} x_1 - \theta_1 & > \eta \\ x_2 - \theta_2 & = -\delta \\ x_3 - \theta_3 & < (\theta_3 - \delta)\, \mathrm{g}(\delta)^{\frac{\gamma_3}{\gamma_2}} - \theta_3 \, (< -\delta) \end{cases}.$$

In this last box the trajectory starting in (x_1, x_2, x_3) is:

$$\begin{cases} x_1(t) = \dfrac{k_1}{\gamma_1} + e^{-\gamma_1 t}\left(x_1 - \dfrac{k_1}{\gamma_1}\right) \\ x_2(t) = \dfrac{k_2}{\gamma_2} + e^{-\gamma_2 t}\left(x_2 - \dfrac{k_2}{\gamma_2}\right) \\ x_3(t) = \dfrac{k_3}{\gamma_3} + e^{-\gamma_3 t}\left(x_3 - \dfrac{k_3}{\gamma_3}\right) \end{cases}.$$

Let $t_6 = \dfrac{-1}{\gamma_3} \ln\left(\dfrac{\frac{k_3}{\gamma_3} - \theta_3 + \delta}{\frac{k_3}{\gamma_3} - x_3}\right)$ the time for which we have $x_3(t) - \theta_3 = -\delta$. For such a time t_6 we have:

$$x_1(t_6) - \theta_1 > \eta,$$

since the function $x_1(t)$ is increasing in t in this box. Lastly decreasing the value of δ if necessary, i.e taking $0 < \delta < \delta_0$ where $0 < \delta_0 < \min_{i=1,2}(\delta_i, \delta_i', \delta_3, \delta_4)$ is chosen small enough, we get:

$$\begin{aligned} x_2(t_6) - \theta_2 &> \frac{k_2}{\gamma_2} - \theta_2 - \left(\frac{\frac{k_3}{\gamma_3} - \theta_3 + \delta}{\frac{k_3}{\gamma_3} - (\theta_3 - \delta)\,\mathrm{g}(\delta)^{\frac{\gamma_3}{\gamma_2}}}\right)^{\frac{\gamma_2}{\gamma_3}} \left(\frac{k_2}{\gamma_2} - \theta_2 + \delta\right) \\ &> \delta. \end{aligned}$$

In this last step we have crossed the boxes B_{210} and B_{220} to reach B_{221}. As a consequence, from our six steps $(i), (ii), (iii), (iv), (v), (vi)$ above, we have proved that there exists a real $0 < \delta_0 < \min_{i=1,2,3}\left(\theta_i, \dfrac{k_i}{\gamma_i} - \theta_i, 1\right)$ such for any $0 < \delta < \delta_0$, any initial trajectory starting in the rectangle $(\mathcal{P})$ follows the cycle $\mathcal{C}$ and returns in $(\mathcal{P})$, as claimed. ■

REFERENCES

[1] R. Casey, H. De Jong, and J.-L. Gouzé, *Piecewise-linear models of genetic regulatory networks: Equilibria and their stability*, Journal of Mathematical Biology, 52 (2006), pp. 27–56.

[2] M. Chaves and M. Preto, *Hierarchy of models: From qualitative to quantitative analysis of circadian rhythms in cyanobacteria*, Chaos, 23 (2013).

[3] M. Davidich and S. Bornholdt, *The transition from differential equations to boolean networks: A case study in simplifying a regulatory network model*, Journal of Theoretical Biology, 255 (2008), pp. 269–277.

[4] R. Edwards, *Analysis of continuous-time switching networks*, Physica D: Nonlinear Phenomena, 146 (2000), pp. 165–199.

[5] M. B. Elowitz and S. Leibler, *A synthetic oscillatory network of transcriptional regulators*, Nature, 403 (2000), pp. 335–338.

[6] E. Farcot and J.-L. Gouzé, *Periodic solutions of piecewise affine gene network models with non uniform decay rates: The case of a negative feedback loop*, Acta Biotheoretica, 57 (2009), pp. 429–455.

[7] ———, *Limit cycles in piecewise-affine gene network models with multiple interaction loops*, International Journal of Systems Science, 41 (2010), pp. 119–130.

[8] A. F. Filippov, *Differential equations with discontinuous right-hand side*, vol. 19 of Mathematics and its Applications, Kluwer Academic Publishers, Dordrecht, Boston, London, 1960.

[9] E. Fung, W. W. Wilson, J. K. Suen, T. Bulter, S.-G. Lee, and J. C. Liao, *A synthetic gene-metabolic oscillator*, Nature, 435 (2005), pp. 118–122.

[10] T. S. Gardner, C. R. Cantor, and J. J. Collins, *Construction of a genetic toggle switch in escherichia coli*, Nature, 403 (2000), pp. 339–342.

[11] T. Gedeon, *Cyclic feedback systems*, Memoirs of the American Mathematical Society, 134 (1998).

[12] ———, *Oscillations in monotone systems with a negative feedback*, SIAM Journal on Applied Dynamical Systems, 9 (2010), pp. 84–112.

[13] T. Gedeon and K. Mischaikow, *Structure of the global attractor of cyclic feedback systems*, Journal of Dynamics and Differential Equations, 7 (1995), pp. 141–190.

[14] L. Glass, *Classification of biological networks by their qualitative dynamics*, Journal of Theoretical Biology, 54 (1975), pp. 85–107.

[15] L. Glass and S. A. Kauffman, *The logical analysis of continuous, non-linear biochemical control networks*, Journal of Theoretical Biology, 39 (1973), pp. 103–129.

[16] L. Glass and J. S. Pasternack, *Prediction of limit cycles in mathematical models of biological oscillations*, Bulletin of Mathematical Biology, 40 (1978), pp. 27–44.

[17] ———, *Stable oscillations in mathematical models of biological control systems*, Journal of Mathematical Biology, 6 (1978), pp. 207–223.

[18] B. C. Goodwin, *Oscillatory behavior in enzymatic control processes*, Advances in Enzyme Regulation, 3 (1965), pp. 425–438.

[19] J. S. Griffith, *Mathematics of cellular control processes i. negative feedback to one gene*, Journal of Theoretical Biology, 20 (1968), pp. 202–208.

[20] S. P. Hastings, *On the uniqueness and global asymptotic stability of periodic solutions for a third order system*, Rocky Mountain Journal of Mathematics, 7 (1977), pp. 513–538.

[21] S. P. Hastings, J. J. Tyson, and D. Webster, *Existence of periodic solutions for negative feedback cellular control systems*, Journal of Differential Equations, 25 (1977), pp. 39–64.

[22] A. Hoffmann, A. Levchenko, M. L. Scott, and D. Baltimore, *The IκB-NFκB signaling module: Temporal control and selective gene activation*, Science, 298 (2002), pp. 1241–1245.

[23] V. I. Istratescu, *Fixed point theory. An introduction.*, Mathematics and Its Applications, Vol. 7. Dordrecht - Boston - London: D. Reidel Publishing Company. XV, 466 p. Dfl. 135.00, 1981.

[24] H. De Jong and J. Geiselmann, *Modeling and simulation of genetic regulatory networks by ordinary differential equations*, Differential Equations, 294 (2003), pp. 766–769.

[25] J. C. Leloup and A. Goldbeter, *Toward a detailed computational model for the mammalian cell clock*, PNAS, 100 (2003), pp. 7051–7056.

[26] L. Lu and R. Edwards, *Structural principles for periodic orbits in glass networks*, Journal of Mathematical Biology, 60 (2010), pp. 513–541.

[27] J. Mallet-Paret and G. R. Sell, *The Poincaré-Bendixson theorem for monotone cyclic feedback systems with delay*, Journal of Differential Equations, 125 (1996), pp. 441–489.

[28] J. Mallet-Paret and H. L. Smith, *The Poincaré-Bendixson theorem for monotone cyclic feedback systems*, Journal of Dynamics and Differential Equations, 2 (1990), pp. 367–421.

[29] T. Mestl, E. Plahte, and S. W. Omholt, *Periodic solutions in systems of piecewise-linear differential equations*, Dynamics and stability of systems, 10 (1995), pp. 179–193.

[30] J. D. Murray, *Mathematical biology*, vol. 19 of Biomathematics, Springer-Verlag, Berlin, 1993.

[31] C. Poignard, *Inducing chaos in a gene regulatory network by coupling an oscillating dynamics with a hysteresis-type one*, Journal of Mathematical Biology, (2013), pp. 1–34.

[32] A. Polynikis, S. J. Hogan, and M. di Bernardo, *Comparing different ode modelling approaches for gene regulatory networks*, Journal of theoretical biology, 261 (2009), pp. 511–530.

[33] J. R. Pomerening, S. Y. Kim, and J. E. Ferrell, *Systems-level dissection of the cell-cycle oscillator: bypassing positive feedback produces damped oscillations*, Cell, 122 (2005), pp. 565–578.

[34] N. Pullen and R. J. Morris, *Bayesian model comparison and parameter inference in systems biology using nested sampling*, PLoS ONE, 9 (2014), p. e88419.

[35] M. J. Rust, J. S. Markson, W. S. Lane, D. S. Fisher, and E. K. O'Shea, *Ordered phosphorylation governs oscillation of a three-protein circadian clock*, Science, 318 (2007), p. 809.

[36] Q. Shu and R. G. Sanfelice, *On the stability of hybrid limit cycles and isolated equilibria in a genetic network with binary hysteresis*, in Decision and Control (CDC), 2013 IEEE 52nd Annual Conference on, Dec 2013, pp. 4080–4085.

[37] H. L. Smith, *Periodic orbits of competitive and cooperative systems*, Journal of Differential Equations, 65 (1986), pp. 361–373.

[38] M. Tigges, T. T. Marquez-Lago, J. Stelling, and M. Fussenegger, *A tunable synthetic mammalian oscillator*, Nature, 457 (2009), pp. 309–312.

[39] T. Y.-C. Tsai, Y. S. Choi, W. Ma, J. R. Pomerening, C. Tang, and J. E. Ferrell, *Robust, tunable biological oscillations from interlinked positive and negative feedback loops*, Science (New York, N.Y.), 321 (2008), pp. 126–129.

[40] J. J. Tyson, *On the existence of oscillatory solutions in negative feedback cellular control processes*, Journal of Mathematical Biology, 1 (1975), pp. 311–315.

[41] J. J. Tyson, K. C. Chen, and B. Novak, *Sniffers, buzzers, toggles and blinkers: dynamics of regulatory and signaling pathways in the cell*, Current Opinion in Cell Biology, 15 (2003), pp. 221–231.

[42] A. Veliz-Cuba, B. Aguilar, F. Hinkelmann, and R. Laubenbacher, *Steady state analysis of boolean molecular network models via model reduction and computational algebra*, BMC Bioinformatics, 15 (2014).

[43] A. Veliz-Cuba, A. Kumar, and K. Josić, *Piecewise linear and boolean models of chemical reaction networks*, Bulletin of Mathematical Biology, 76 (2014), pp. 2945–2984.